IMPROVEMENT OF BIOFUEL FERMENTATION PROCESSES WITH USE OF POLY(VINYLDODECYLIMIDAZOLIUM BROMIDE) FOR *IN-SITU* PRODUCT REMOVAL

by

Rachel Helen Vincent

A thesis submitted to the Department of Chemical Engineering

In conformity with the requirements for

the degree of Master's of Applied Science

Queen's University

Kingston, Ontario, Canada

(December, 2018)

Abstract

The production of biofuels through fermentation has become increasingly important due to the need for sustainable energy sources. The fermentation processes of ethanol and *n*-butanol, by *Saccharomyces cerevisiae* and *Clostridium acetobutylicum*, respectively, suffer from end-product inhibition, hindering final product concentrations, volumetric productivity, and product recovery. To alleviate these limitations, *in-situ* product removal (ISPR) methods can be implemented, via two-phase partitioning bioreactor (TPPB) technology. This work used a polyelectrolyte absorbent phase, poly(vinyldodecylimidazolium bromide) [P(VC_{12}ImBr)], in TPPB systems for the removal of the target molecules, ethanol and *n*-butanol, with focus on the latter due to more severe product inhibition and its greater promise as a biofuel.

P(VC_{12}ImBr) was synthesized and characterized for ISPR implementation and was found to have a partition coefficient (PC) and selectivity of 1.1 and 7.2 for ethanol, and a PC of 6.5 and selectivity of 46 for *n*-butanol. Characteristics of P(VC_{12}ImBr) were found to be favorable for TPPB implementation, including its density, diffusivity for *n*-butanol, and complete biocompatibility with *S. cerevisiae* and *C. acetobutylicum*. A differential scanning calorimetry (DSC) scan of P(VC_{12}ImBr) found its melting temperature to be -17°C and a glass transition temperature above 200°C, which can be reduced by plasticization with water. Anion exchange between bromide in P(VC_{12}ImBr) and sulphate and phosphate ions in fermentation medium was observed, however this did not affect its PC or selectivity.

When implemented in ethanol and acetone-butanol-ethanol (ABE) ISPR fermentations, P(VC_{12}ImBr) absorbed target molecules from the fermentation broth, however improvements relative to a control were observed only for the ABE fermentation with the mass fraction of sorbent used. In the ABE ISPR fermentation there was greater substrate conversion and an increase in volumetric productivity of 76%.

The water + *n*-butanol + P(VC_{12}ImBr) ternary system confirmed P(VC_{12}ImBr)'s preference for *n*-butanol by concentrating dilute solutions above its aqueous solubility limit. To examine *n*-butanol absorbed by P(VC_{12}ImBr), a 1.5 wt% *n*-butanol solution was concentrated to 25 wt% *n*-butanol, which was thermally removed and condensed to show phase separation. The ability of P(VC_{12}ImBr) to concentrate dilute solutions of *n*-butanol above its solubility limit would allow for an improved *n*-butanol purification process.

Acknowledgements

I would like to thank my supervisor, Dr. Andrew Daugulis for granting me the opportunity to perform research in his lab. His consistent encouragement and patience were greatly appreciated throughout the completion of this thesis. I would also like to thank Dr. Scott Parent for his technical expertise in polymer synthesis and characterization. As well, I would like to thank Nathan Mullins and Rob Biro for helping me in the lab.

Table of Contents

List of Figures

List of Tables

Chapter 1

Introduction

1.1 Background

The desire to reduce carbon dioxide emissions in North America has led to increased efforts to provide environmentally sound energy sources. In particular, transportation fuel alternatives are a focus, specifically the generation of sustainable biofuels to replace petroleum-based gasoline (Qureshi & Ezeji, 2008). Biofuels, which are produced biologically through fermentation processes, have been a focus of energy initiatives by both the Canadian and U.S. governments and as a result are being pursued by industry and researchers (Natural Resources Canada 2016; U.S. EPA 2018). Initial biofuel production focused on ethanol due to its established reputation, however *n*-butanol has become a new focus due to its advantages over ethanol as a transportation fuel (Jin et al. 2011; Qureshi & Ezeji, 2008).

Ethanol and *n*-butanol can be produced through fermentation processes involving *Saccharomyces cerevisiae* and *Clostridium acetobutylicum*, respectfully. Unfortunately, end-product inhibition is a common feature within these fermentation processes, as the desired products are toxic to the microorganisms themselves, resulting in low product yields and low volumetric productivities (Jones & Woods, 1986). Using *S. cerevisiae* in the ethanol fermentation process, the final product concentration generally cannot exceed 12 wt% due to end-product inhibition (Bai et al., 2008), similarly, *n*-butanol, produced by wild strains of *clostridia* in acetone-butanol-ethanol (ABE) fermentation, cannot exceed 2 wt% total solvents due to *n*-butanol toxicity (Jones & Woods, 1986). The dilute product concentration of *n*-butanol, coupled with the formation of a heterogeneous azeotrope, makes the downstream recovery of *n*-butanol particularly challenging, as two distillation columns are required for purification (Matsumura et al., 1988; Oudshoorn et al., 2009). As low aqueous product concentrations are an obstacle that limits these fermentation

processes, *in-situ* product removal strategies can be implemented to alleviate the effects of end-product inhibition (Daugulis, 1988).

The use of *in-situ* product removal (ISPR) technologies in ethanol and ABE fermentation processes have shown improvements in the overall production of ethanol and *n*-butanol via extraction of the inhibitory products throughout the fermentation, reducing toxic product concentrations leading to enhanced production and greater volumetric productivities (Daugulis, 1988), along with advantages in downstream processing (Matsumura et al., 1988). Two-phase partitioning bioreactors (TPPBs) are an ISPR technology that have been proven effective for ethanol and ABE fermentation processes, as they incorporate a second phase with a high affinity for the target molecule, a property assessed by its partition coefficient (PC). Initial TPPB work involved the use of water-immiscible organic solvents to reduce toxic solvent concentrations within a fermentation medium, however the focus has recently shifted to the use of solid sequestering phases due to several advantages including excellent partitioning capabilities, complete biocompatibility, and ease in handling due to mechanical stability (Dafoe & Daugulis, 2014).

Recent work by Bacon et al. (2017) involved the development and evaluation of solid absorbent polyionic liquids (PILs) for their PC and selectivity (α), a measure of the preference for sequestering a target molecule over water. Results showed that many of these novel PILs have a high affinity for *n*-butanol and other fermentation products, including ethanol and acetone, and coupled with their mechanical advantages as solid polymers, have immense potential for use as a partitioning phase in a TPPB fermentation system and subsequent recovery processes. This provides an opportunity to further investigate and define PIL absorbent characteristics to implement in a TPPB system for fermentation and recovery improvements.

1.2 Objectives

The purpose of this work was to improve biofuel fermentation and recovery processes using poly(vinyldodecylimidazolium bromide) [P(VC_{12}ImBr)], an absorbent PIL, in solid-liquid

TPPB systems, with a main focus on the production of *n*-butanol in an ABE fermentation. The first objective was to characterize P(VC_{12}ImBr) for its use in biofuel fermentation processes. The next objective was to reduce product inhibition and improve the biofuel fermentations using P(VC_{12}ImBr) to absorb toxic fermentation products *in situ*. Finally, the recovery of *n*-butanol from P(VC_{12}ImBr) was investigated for improving the *n*-butanol purification process.

1.3 References

Bacon, S.L., Ross, R.J., Daugulis, A.J., & Parent, J.S. (2017). Imidazolium-based polyionic liquid absorbents for bioproduct recovery. *Green Chemistry, 19*(21), 5203-5213.

Bai, F. W., Anderson, W. A., & Moo-Young, M. (2008). Ethanol fermentation technologies from sugar and starch feedstocks. *Biotechnology Advances*, *26*(1), 89–105.

Dafoe, J. T., & Daugulis, A. J. (2014). *In situ* product removal in fermentation systems: Improved process performance and rational extractant selection. *Biotechnology Letters*, *36*(3), 443–460.

Daugulis, A.J. (1988). Integrated reaction and product recovery in bioreactor systems. *Biotechnology Progress*, *4*(3), 113-122.

Jin, C., Yao, M., Liu, H., Lee, C. F. F., & Ji, J. (2011). Progress in the production and application of *n*-butanol as a biofuel. *Renewable and Sustainable Energy Reviews*, *15*(8), 4080–4106.

Jones, D. T., & Woods, D. R. (1986). Acetone-butanol fermentation revisited. *Microbiological Reviews*, *50*(4), 484–524.

Matsumura, M., Kataoka, H., Sueki, M, & Araki, K. (1988). Energy saving effect of pervaporation using oleyl alcohol liquid membrane in butanol purification. *Bioprocess Engineering, 3*(2), 93-100.

Natural Resources Canada. (2016). Ethanol. Retrieved from http://www.nrcan.gc.ca/energy/alternative-fuels/fuel-facts/ethanol/3493#a7

Oudshoorn, A., van der Wielen, L.A.M, & Straathof, A.J.J. (2009). Assessment of options for selective 1-butanol recovery from aqueous solution, *Industrial & Engineering Chemistry Research, 48*(15), 7325-7336.

Qureshi, N., & Ezeji, T.C. (2008). Butanol, 'a superior biofuel' production from agricultural residues (renewable biomass): recent progress in technology. Biofuels, Bioproducts and Biorefining, *2*(4), 319-330.

United States Environmental Protection Agency. (2018). Renewable Fuel Standard Program. Retrieved from https://www.epa.gov/renewable-fuel-standard-program

Chapter 2

Literature Review

2.1 Introduction

Over the past few decades, the depletion of fossil fuels and their harmful effects on the environment have led to a global push towards the use of renewable energy sources with sustainable production methods (Hatti-Kaul et al., 2007; Jin et al., 2011). This drive stems from societal motivation, alongside government policies, such as fines and taxation on pollution and waste disposal, which have been introduced to reduce our reliance on non-renewable fossil fuels (Hatti-Kaul et al., 2007; Kamm & Kamm, 2004). Among the hydrocarbon-dependent areas that need to be modified for sustainability, transportation energy sources have become a target as they account for a substantial percentage of energy consumption, due to both the sourcing of fuel sources, along with carbon emissions produced from combustion of the fuel itself (Antoni et al., 2007). In addition to negative environmental impacts, transportation fuels have an international prevalence and their continued growth as a sector deems them as an objective for increased attention (Antoni et al., 2007; Qureshi & Ezeji, 2008).

To reach specific emission targets in North America, mandates have been set out by both Environment Canada and the United States Environmental Protection Agency, requiring gasoline to contain up to 10% of an oxygenate additive (Natural Resources Canada, 2016; United States Environmental Protection Agency, 2018). Along with reducing dependence on fossil fuels, the mandatory addition of an oxygenate to gasoline reduces carbon monoxide production, allowing for cleaner fuel combustion. Both ethers and alcohols were initially used as oxygenates, with the focus having shifted to the latter due to the environmental and health concerns associated with ethers, along with the notion that alcohols can be produced from renewable resources (United States Environmental Protection Agency, 2018). Therefore, the sustainability of biologically produced

alcohols led to the wide-spread production of ethanol on an industrial scale, as its fermentative production is a well-known bioprocess (Bai et al., 2008).

In addition to incentives for producing bio-based fuels, governments have encouraged the production of alternative biobased products, as seen in the National Research Council (NRC) of the United States' report "Biobased Industrial Products: Priorities for Research and Commercialization," which highlights the benefits of biobased industrial products to encourage displacement of hydrocarbon-based processes (Dale, 2003). Based on these government initiatives, along with the U.S. Department of Energy's goal to replace 30% of transportation fuels and 25% of industrial organic chemicals by 2025 with biofuels and products derived from biomass (Ragauskas et al., 2006), there will be a reduced need for non-renewable carbon resources (Dale, 2003; National Research Council, 2000). This is supplemented by a strong trend in the use of biofuels, as international biofuel production has increased more than fivefold between 2001 and 2012 (Kujawska et al., 2015). Furthermore, Kamm and Kamm (2004) emphasize the growth of renewable biorefinery processes, including the fermentative production of bioproducts, as they have become recognized as effective alternatives to lessen the dependence on non-renewable resources.

2.2 Biofuels and their Fermentation Processes

Ethanol, along with diesel and *n*-butanol, can be produced biologically and derived from biomass sources, including plants and other organic matter, which categorizes them as "biofuels" (Jin et al., 2011; Naik et al., 2010). These biofuels are chemically identical to petroleum-based or synthetically produced ethanol, diesel, and *n*-butanol, however based on their source, may have "bio" as a prefix to be bioethanol, biodiesel, or biobutanol. Bioethanol and biobutanol are produced through the fermentation of sugars derived from biomass, whereas biodiesel is produced through transesterification of biomass (Naik et al., 2010). Compared to traditional petroleum-derived fossil fuels, biofuels are a renewable energy source because the feedstocks involved in biofuel production

are ultimately derived from living plants, and when combusted, the carbon dioxide emitted can be photosynthetically taken up by plants for their growth, which largely ameliorates the possibility of increasing atmospheric carbon dioxide levels (Naik et al., 2010; Kamm & Kamm, 2004).

Ethanol produced through fermentation industrially is considered to be a 'first generation' biofuel. This classification is based on the biomass utilized in production, which can be derived from food source biomass materials such as corn, wheat or sugarcane crops. Though considered sustainable, 'first generation' biofuels are of concern due to the 'food versus fuel' debate, in which it is argued that the use of food crops as a biofuel feedstock leads to increased deforestation for workable land, along with higher food prices, which has a specific negative impact in parts of the developing world (Fairley, 2011; Naik et al., 2010). Addressing the concerns associated with 'first-generation' biofuels is a category of biofuels known as 'next-generation' biofuels, which utilize non-food biomass as feedstock, including lignocellulosic biomass and crop wastes. The 'next generation' category of biofuels is also noted to have properties superior to the commonly produced ethanol, such as *n*-butanol, which contains a higher energy content amongst other beneficial qualities (Atsumi et al., 2008), as described later.

Biological fermentation is a process in which a saccharide substrate, typically glucose, is consumed by a microorganism and transformed through a metabolic pathway to produce the biochemical end-products (Kujawska et al., 2015; Najafpour et al., 2004). Ethanol and *n*-butanol fermentation processes vary according to operating conditions including oxygen requirement, agitation, temperature, and pH, as well as the microorganism involved. The microbial strain can have an influence both on the rate and the amount of alcohol produced, important aspects for determining the economic viability of the process (Staggs & Nielsen, 2015).

2.2.1 Ethanol Fermentation Processes and Applications

The ethanol fermentation process has a long history, as producing this alcohol for consumption dates back to around 7000 BCE (McGovern et al., 2004). The use of ethanol as a

biofuel is much more recent, as production for this purpose began in the 1970s due to the recognition that fossil fuel reserves are finite, along with a steep 350% increase in oil price (Bai et al., 2008; Maiorella, 1985; Najafpour et al., 2004). Alongside the previously mentioned government incentives, and coupled with consumption-based industries, the commercial production of ethanol as a biofuel was emphasized due to its well-known process characteristics.

Ethanol fermentation most commonly involves the use of the yeast species *Saccharomyces cerevisiae*, also known as Baker's or Brewer's yeast, due to its multiple applications (Najafpour et al., 2004). Bai et al. (2008) describes the ethanol fermentation process, in which *S. cerevisae* performs glycolysis via the Embden-Meyerhof-Parnas (EMP) pathway. Following the EMP pathway, one molecule of glucose is consumed to produce two molecules of ethanol and two molecules of carbon dioxide (CO_2). The production of CO_2 alongside ethanol is not desirable in a biofuel context, however is essential for beer or wine-making and baking processes, as carbonation is desired for flavour and leavening of these consumables. In addition, the EMP pathway produces two molecules of ATP to provide energy, which contribute to biomass production.

$$C_6H_{12}O_6 \rightarrow 2\ C_2H_5OH\ (ethanol) + 2\ CO_2 + 2\ ATP \quad \textbf{(2.1)}$$

Although ethanol is the most commonly produced biofuel on an industrial scale, there are drawbacks associated with its application as an effective oxygenate. As ethanol has a lower energy content compared to conventional fuels and other biofuels, it generally cannot be combined with gasoline or diesel at concentrations over 10% as an effective and sustainable replacement (Natural Resources Canada, 2016; Jin et al., 2011). There are also drawbacks associated with ethanol's high hydrophilicity, and since there is high risk with water attraction, it cannot be transported through existing pipelines.

2.2.2 *n*-Butanol Fermentation Processes and Applications

n-Butanol is produced biochemically through acetone-butanol-ethanol (ABE) fermentation, which was discovered in 1861 by Louis Pasteur (Ndaba et al., 2015). The isomer *n*-

butanol is the main end product accumulated through ABE fermentation, along with smaller amounts of acetone and ethanol, at a 6:3:1 ratio (Jin et al., 2011, Kujawska et al., 2015). The metabolic conversion process of ABE fermentation occurs through the utilization of *Clostridium* bacterial strains, most commonly the wild type *Clostridium acetobutylicum*.

A standard batch fermentation utilizing *C. acetobutylicum* undergoes two distinct phases, acidogenesis and solventogenesis. Acidogenesis occurs with initial cell growth to produce acetic acid and butyric acid, along with hydrogen and carbon dioxide gases. Acetone, *n*-butanol, and a small amount of ethanol are then produced in the solventogenesis phase of the ABE fermentation (Jones and Woods, 1986).

n-Butanol's potential as a biofuel has drawn increased interest in recent years, with properties as a sustainable biofuel that are superior to ethanol. Because of *n*-butanol's longer carbon chain, it has a higher energy content compared to ethanol, which leads to better mileage, an undisputed quality in a transportation fuel. *n*-Butanol also has higher miscibility with gasoline and diesel compared to ethanol, which is essential in the integration of a biofuel with currently used hydrocarbon fuels. *n*-Butanol's higher viscosity is also more suitable in diesel engines, as it has a higher miscibility with diesel fuel for minimal phase separation. In addition, *n*-butanol can be more safely transported and stored in existing fuel infrastructure due to its hydrophobicity (Jin et al., 2011). Finally, *n*-butanol has a higher boiling point than ethanol, which influences its volatility, preventing vapour lock that may arise in the warmer summer months. These features highlight *n*-butanol's compatibility with gasoline and diesel as a preferable biofuel and are summarized in Table 2.1.

Along with *n*-butanol, isobutanol is a branch-chained isomer of interest as a biofuel as its properties are considered to be even more impressive than *n*-butanol. Isobutanol's structure allows it to have a higher energy content than ethanol, higher viscosity than *n*-butanol, and is even less miscible with water, contributing to its usefulness as a biofuel. Although it cannot be produced by

wild strains of microorganisms, it is currently being produced industrially by Butamax and Gevo, with the utilization of genetically modified microorganisms to specifically produce comparably higher concentrations of isobutanol (Butamax, 2018; Gevo 2018).

Table 2.1: Properties of conventional fuels and biofuels

	Gasoline	**Diesel**	**Ethanol**	***n*-Butanol**	**Isobutanol**
Structure	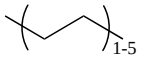	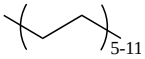	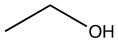	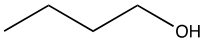	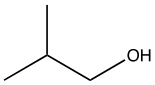
Carbon Chain	C_4-C_{12}	C_{12}-C_{25}	C_2	C_4	C_4
Energy content (MJ/kg)	43	43	27	33	33
Density at 20°C (g/L)	720-780	820-860	790	810	802
Viscosity at 40°C (cSt)	0.4-0.8	1.9-4.1	1.1	2.6	4.3
Solubility of water (wt%)	0	<0.02	100	20	15
Boiling Point (°C)	100-400	180-360	78	117	107

Note: Information is from Jin et al. (2011).

2.2.3 End-Product Inhibition in Fermentation Processes

Although biofuel fermentation processes are more environmentally sustainable than chemical routes to produce transportation fuels, they are limited as economically viable processes due to low product titers. This drawback is a result of end-product inhibition in both ethanol and ABE fermentation processes, an unavoidable effect in which the alcohol end-products are toxic to the microorganisms in use (Daugulis, 1988). End-product inhibition begins at an alcohol concentration specific to the fermentation process, at which microorganism growth and product formation begins to slow down, and eventually ceases altogether. Ultimately, this effect leads to low final product concentrations (g/L) and volumetric productivities (g/Lh), which quantitatively

determine the economic viability and effectiveness of a fermentation process. It is also reflected in product recovery costs for the separation of the dilute product through distillation.

For *S. cerevisiae* in an ethanol fermentation, inhibitory effects begin to be seen at an ethanol concentration around 30 g/L, ultimately producing a maximum 120 g/L or approximately 12 wt% final ethanol concentration (Bai et al., 2008; Kollerup & Daugulis, 1985; Lin & Tanaka, 2006). ABE product inhibition is more severe, as *n*-butanol is extremely toxic even at low concentrations, (Jones & Woods, 1986; Linden et al., 1985). Once the *n*-butanol threshold concentration is reached at about 3.7 g/L, growth inhibition begins to be observed (Linden et al., 1985), and due to this toxicity, total ABE production can only reach a maximum of 20 g/L or about 2 wt% (Jones & Woods, 1986). As ethanol and *n*-butanol toxicity severely inhibits the potential for biofuel fermentation processes and their associated environmental and economic advantages, it is desirable to determine ways in which the inhibition can be mitigated.

2.3 *In-situ* Product Removal to Improve Biofuel Fermentation Processes

Fermentation processes which suffer from end-product inhibition, such as in the production of ethanol and *n*-butanol, have become the subject of multiple experimental approaches to improve production, creating more efficient processes to ultimately reduce costs (Bai et al., 2008; Kujawska et al., 2015). Methods for fermentation process improvement that have been implemented include microbial strain modification and engineering, substrate alteration, enhanced bioreactor design, and the focus of this research: *in-situ* product removal (Jin et al., 2011).

In-situ product removal (ISPR) is a concept that involves selective removal of the inhibitory product within a fermentation process as the fermentation progresses (Roffler et al., 1987a; Xue et al., 2014). ISPR techniques have been shown to minimize the effects of product toxicity through its integrated removal within a bioreactor, which in turn increases the effective final product concentration and volumetric productivity of a fermentation process (Dafoe & Daugulis, 2014). In addition, ISPR can improve solvent recovery by selective removal of target

molecules for easier downstream processing, and potentially concentrate it. Common ISPR techniques tested include gas stripping for volatile products, selective permeation membranes for pervaporation and perstraction, and two-phase partitioning bioreactor configurations, which can be applied regardless of a product's relative volatility (Dafoe & Daugulis, 2014; Outram et al., 2017; Xue et al., 2014). Though experimental results have demonstrated that ISPR can improve fermentation process outcomes, the effectiveness of each method will be described in this section (Dafoe & Daugulis, 2014; Staggs & Nielsen, 2015).

2.3.1 Gas Stripping

This method involves the separation of volatile target molecules from the fermentation broth with the sparging of gas through the bioreactor, sometimes including recycling the gases produced throughout the process, such as CO_2 and H_2; and the solute vapour is then condensed and later recovered (Kujawska et al., 2015). Although effective at achieving significant final titers, gas stripping can be expensive as it requires a very high energy input compared to other ISPR methods due to low selectivity of gas for the desired products that takes up significant amounts of water, which requires more energy in distillation process (Oudshoorn et al., 2009; Qureshi et al., 2005; Vane, 2008; Xue et al., 2012).

2.3.2 Permeation Membranes

Permeation membrane ISPR techniques, such as perstraction and pervaporation, use a selectively permeable membrane that allows the target molecule to be sequestered away from the fermentation broth within a bioreactor, thereby reducing the toxic product concentration (Kujawska et al., 2015). Permeation membranes through perstraction involve a membrane which separates the bioreactor contents from an organic liquid extractant selected to have a high affinity for the target solute, which sequesters the desired product (Dafoe & Daugulis, 2014; Kujawska et al., 2015; Outram et al., 2017). This differs from pervaporation, in which sequestration is achieved through the application of gas or vacuum on the other side of a separating membrane that is permeable to

the target solute (Outram et al., 2017). Although effective at minimizing product inhibition, perstraction and pervaporation ISPR techniques are limited by the rate of product flow through the membrane barrier, which can decrease volumetric productivity, and can lead to potential membrane fouling (Huang et al., 2014).

2.3.3 Two-Phase Partitioning Bioreactors

Two-phase partitioning bioreactor (TPPB) systems are an innovative ISPR technology in which a second water-immiscible phase is added to the cell-containing aqueous bioreactor phase to extract inhibitory products through sorption (Collins & Daugulis, 1996; Dafoe & Daugulis, 2014; Jones et al., 1993; Poleo & Daugulis, 2014). TPPB configurations are of either liquid-liquid extraction or solid-liquid extraction types, allowing for a range of non-aqueous materials to be considered for use. Ultimately, this *in-situ* technique extends activity of the cells in use through reduced exposure to toxic products, resulting in increased final product concentrations and improved productivity (Dafoe & Daugulis, 2014). Products absorbed by TPPB extractants at high concentrations can also be recovered for downstream processing, which can be purified by distillation more easily (Roffler et al., 1984; Xue et al., 2012).

2.4 Considerations for ISPR with the Application of TPPB Systems

Various liquid and solid materials have been implemented as sequestering phases in TPPB systems, including water-immiscible organic solvents and liquid polymers, as well as solid adsorbents as has previously been described and reviewed (Dafoe & Daugulis, 2014; Outram et al., 2017; Vane, 2008). The sequestering phases used in a TPPB system must be completely biocompatible and non-bioavailable, and their effectiveness is governed by their affinity, selectivity, sorption mechanism, and rate of uptake for desired target molecules. Alongside these properties, Dafoe & Daugulis (2014) recommend that, for utmost process improvement, it is imperative that the phase also allows for easy downstream separation, ease of handling, low

volatility and flammability, and economic viability. These factors that deem a material effective for a TPPB system will be described in this section.

2.4.1 Partition Coefficient and Selectivity

The affinity of a sequestering phase for a target molecule is determined through finding the solute concentration before and after equilibrium in the system has been reached. For most materials that are used in TPPB systems, this is described by the dimensionless partition coefficient (PC) (Staggs & Nielsen, 2015; Poleo & Daugulis, 2014), as:

$$PC_i = \frac{w_i^e}{w_i^{aq}} \tag{2.2}$$

where w_i^e is the weight fraction of the target molecule in the extractant phase, and w_i^{aq} is the weight fraction of the target molecule in the aqueous phase, both at equilibrium. A higher PC is desired in TPPB systems, as less extracting material is required for effective sequestering, associated with reduced overall bioreactor volume, enhancing the volumetric productivity and lowering the operating costs of a process (Dafoe & Daugulis, 2014; Vane, 2008).

While the PC encompasses the affinity of the extractant phase for the target molecule, selectivity is a measure of an extractant's preference for the target molecule over water (Bruce & Daugulis, 1991; Dafoe & Daugulis, 2014; Jones et al., 1993; Vane, 2008). Like the PC of a material, selectivity is also dimensionless and used to quantify the desirable properties of an extractant, defined as:

$$\alpha_{i/w} = \frac{PC_i}{PC_w} \tag{2.3}$$

where PC_i is the partition coefficient of the target molecule into the extractant phase, and PC_w is the partition coefficient of water (Dafoe & Daugulis, 2014). Selectivity characterizes the ability of a phase to preferentially remove the target molecule over water. A high selectivity results in a higher final product concentration in the extractant, which reduces further downstream processing costs (Bacon et al., 2017; Dafoe & Daugulis, 2014; Vane, 2008).

2.4.2 Biocompatibility and Non-bioavailability

Along with a high affinity and high selectivity, a successful TPPB system needs its sequestering phase to be biocompatible and non-bioavailable. For a secondary phase material to be deemed biocompatible in a TPPB system, it must not inhibit the growth of an organism, such as *S. cerevisiae* or *C. acetobutylicum* (Bruce & Daugulis, 1991). Biocompatibility testing can be accomplished in two ways, including cell density counts for cell growth (Bacon et al., 2017) and glucose conversion measurements for cell metabolism (Mao et al., 2013), which have been previously described. The bioavailability of the sequestering phase describes whether a microorganism will consume it as a carbon source and is characterized by cell growth in the presence of an extractant (Macleod & Daugulis, 2003). A non-bioavailable sequestering phase is necessary as it ensures that it will not act as an energy source for microorganism growth and thus act only as an extractant to remove fermentation products, without required continuous addition for ISPR (Dafoe & Daugulis, 2014; Macleod & Daugulis, 2003).

2.4.3 Rate of Uptake and Diffusivity

The rate of uptake and diffusivity of a target molecule by an extractant impact the effectiveness of polymers in solid-liquid TPPB systems (Fam & Daugulis, 2012). Therefore, consideration for solute sequestration in solid polymers includes both external mass transport, as well as internal diffusion of the solute into the sequestering phase, and must not be limited by these sorption mechanisms (Amsden et al., 2003; Fam & Daugulis, 2012). As the extracting phase in a TPPB system needs to take up the product at a rate that is comparable to or faster than the biological rate of the microorganism in use, rapid sequestration needs to occur prior to the introduction of inhibitory alcohol levels, which also leads to the consideration of using a material with a diffusivity value which does not limit the system (Fam & Daugulis, 2012; Pittman et al., 2015).

2.5 Ethanol and ABE Fermentation TPPB Systems

Selection of appropriate extractants for use in TPPB systems has improved through research of the above-mentioned considerations for many important bioprocesses including applications in bioproduction and biodegradation (Dafoe & Daugulis, 2014). Ethanol and ABE fermentation processes have benefited from TPPB technology, as implementation can result in increased final product concentrations and volumetric productivities, the defined measures of success in this area. The following section describes the various materials which have been used previously and achieved impressive results with liquid-liquid and solid-liquid TPPB systems for ethanol and ABE fermentation processes, a summary of which can be seen in Table 2.2 and Table 2.3, respectively.

Table 2.2: Previous results for ethanol fermentations with various ISPR methods

ISPR Extractant	Mode	EtOH Productivity (g/Lh)	Total EtOH Produced (g/L)	Source
None	Batch	1.85	94.0	Zhao et al., 2014
CO_2	Fed-batch	8.6	136.9	Sonego et al., 2018
Oleyl alcohol	Fed-batch	0.96	152.8	Jones et al., 1993
Dowex Optipore L-493	Batch	n/a	58	Daugulis & Milton, 2012
Oleyl alcohol	Continuous	32.7	68	Daugulis et al., 1994

Note: Total ethanol produced is based on the total amount of ethanol per aqueous phase volume of bioreactor.

Table 2.3: Previous results for ABE fermentations with various ISPR methods

ISPR Extractant	Mode	*n*BuOH Productivity (g/Lh)	Total *n*BuOh Produced (g/L)	Reference
None	Batch	0.24	19.1	Xue et al., 2012
CO_2 and H_2	Fed-batch	0.35	113.24	Xue et al., 2012
Oleyl alcohol in benzyl benzoate	Batch	0.74	19.3	Roffler et al., 1987b
Polyvinylpyradine resin	Batch	0.42	17.5	Yang, et al., 1994
Oleyl alcohol	Fed-batch	1.0	40	Roffler et al., 1988

Note: Total *n*-butanol produced is based on the total amount of *n*-butanol produced per aqueous phase volume of bioreactor.

2.5.1 Liquid-Liquid TPPB Systems

Ethanol fermentations have long been the focus of research in process improvement with liquid-liquid extractive fermentation systems, with research beginning in the early 1980s focusing on the use of immiscible organic solvents (Kollerup & Daugulis, 1985; Minier & Goma, 1982; Van Hecke et al., 2014). This initial work commonly involved the use of dodecanol or oleyl alcohol as the extractant phase in TPPB systems for ethanol fermentations, as they had demonstrated successful sequestration of the target molecule, along with being both biocompatible and non-bioavailable (Kollerup & Daugulis, 1985; Minier & Goma, 1982). However, there were difficulties associated with use of dodecanol in a stirred-tank bioreactor with standard operating conditions for a fermentation, including emulsion-forming tendencies, high solubility in water, and a low melting point of 26°C (Kollerup & Daugulis, 1985). These organic solvents, among others, have also been studied for use in ABE fermentation TPPB systems for *n*-butanol sequestration, however undesirable bioreactor operational issues are still present, including difficultly in the handling of liquids and recovery of target molecules, along with generally low partitioning of the target molecule by the extractant (Barton & Daugulis, 1992; Dafoe & Daugulis, 2014; Outram et al., 2017; Van Hecke et al., 2014).

In more recent years, liquid-liquid TPPB technology research has led to increased investigation into ionic liquids, as they fit specific characteristics that are advantageous for product recovery, including a high affinity and selectivity for target molecules. Ionic liquids have also become of interest as extractants as they are customizable, allowing them to be tailored to fit specific needs in a fermentation as a material with desirable sorption capabilities (Bacon et al., 2016; Dafoe & Daugulis, 2014). Though many ionic liquids have both high PCs and selectivity as extractants for target molecules, there are problems regarding their biocompatibility, as most ionic liquids are toxic to many microorganisms, including *S. cerevisiae* and *C. acetobutylicum* (Bacon et al., 2016; Cascon et al., 2011; Dafoe & Daugulis, 2014; Jiménez-Bonilla & Wang, 2017).

2.5.2 Solid-Liquid TPPB Systems

Solid polymers became of interest in TPPB systems as they encompass many desirable qualities for biphasic systems that lead to superior performance compared to liquid extractants. These advantages include complete biocompatibility and non-bioavailability, as well as ease of use, given that solid polymers are anticipated to be chemically stable and non-volatile secondary phases (Dafoe & Daugulis, 2014; Parent et al., 2012; Qureshi et al., 2005). Solid extractants in TPPB systems are either adsorbent or absorbent materials, differing by their sorption mechanism, which in turn affects their ISPR abilities.

Adsorbent polymers are specifically engineered to have large surface areas that consist of highly crosslinked rigid, macroporous beads, and are therefore hard, glassy materials, which govern their sequestration abilities within a TPPB (Nielsen & Prather, 2009). However, there are several problems regarding the effectiveness for use within a TPPB due to the physical properties of adsorptive resin surfaces. As the surface of adsorptive polymers have only a specific number of sites for sorption, there is competition amongst the target molecule and other solutes within the fermentation medium, resulting in limited effective sequestering (Mirata et al., 2009). Additional concerns with high surface area polymers include the potential for biofilm formation and fouling

by cells, as well as mechanical failure that damages the polymer structure, which reduces adsorption capacity within the system (Mirata et al., 2009; Nielsen & Prather, 2009; Wang et al., 2012). These concerns are specific to adsorptive polymers, which lead to investigation into the implementation of absorptive polymers (Dafoe & Daugulis, 2014).

The use of absorptive polymers in TPPB systems can be more appealing compared to adsorbent materials as they are generally more effective in sequestering specific target molecules, including alcohols, due to their sorption mechanism, in addition to having other property-based advantages including mechanical toughness, adjustable selectivity, reduced bio-fouling, and lower cost (Dafoe & Daugulis, 2014). Many absorptive polymers used in TPPB systems are semi-crystalline, containing a crystalline section with a melting temperature (T_m) and an amorphous section with a glass transition temperature (T_g), the points above which changes their properties to be soft and amorphous and improves solute uptake (Bacon et al., 2015; Parent et al., 2012). However, when a semi-crystalline polymer is heated above its T_m, melting means that the crystalline sections of the polymer fall out of their structure, and not that the polymer transitions to a liquid state (Bunn, 1955). Successful semi-crystalline absorbents have a T_m and T_g that are lower than the bioreactor operating temperature, which allow for better absorption and permeation of a solute into the material (Bacon et al., 2015; Parent et al., 2012; Poleo & Daugulis, 2014). However, materials with a high T_g can be plasticized with water to improve solute absorption (Parent et al., 2012).

Included in the category of absorbent materials are solid polyionic liquids (PILs), which are polymerized ionic liquids, and a class of polyelectrolyte materials (Bacon et al., 2017; Yuan & Antonietti, 2011). PILs have the potential to be advantageous as extractants in TPPB systems as they have a high affinity and selectivity for target molecules like their ionic liquid precursors, however their composition as polymers mitigates their toxicity towards microorganisms (Bacon et al., 2017).

2.6 Recovery of Products in TPPB Systems

Following the production and extraction of a fermentation product in a TPPB system, effective final product recovery of the biofuels is necessary. In a typical ethanol or ABE fermentation, product recovery and purification involve the use of multiple units, including distillation columns, extraction columns, and decanters (Kujawska et al., 2015; Luyben, 2008; Tao et al., 2014). As product recovery involves energy-intensive steps, simplification of the recovery process is desirable, and can be improved through use of ISPR, with focus on a system's azeotrope and solubility limits.

2.6.1 Ethanol Distillation

During ethanol distillation, the ethanol + water azeotrope is formed at 78.2°C with the mixture consisting of 4.4 wt% water (Rumble, 2018). This azeotropic mixture is homogeneous, as ethanol is completely miscible in water, which is not advantageous in the purification process where water should be removed to the greatest extent. Therefore, various techniques are commonly used to assist with further purification by altering the system's boiling point, including extractive distillation, or molecular sieve dehydration (Kumar et al., 2010).

2.6.2 *n*-Butanol Distillation

The *n*-butanol + water azeotropic system is formed at 92.5°C, consisting of 44.5 wt% water (Rumble, 2018), however it is a heterogeneous azeotrope. *n*-Butanol's solubility in water and the solubility of water in *n*-butanol are listed in Table 2.4. The condensation of any concentration of *n*-butanol above 7.3 wt%, such as that of the azeotrope, will result in two liquid phases present at equilibrium, one aqueous water-rich phase at the solubility limit, and one organic *n*-butanol-rich phase (Matsumura et al., 1988). This heterogeneous azeotrope requires a two-column system to be used, which is seen in Figure 2.1. In this setup, a feed flows into the first column, where *n*-butanol and water vaporize as the mixture approaches its *n*-butanol azeotropic composition of 55.5 wt%. The *n*-butanol-water vapor is then condensed and sent to the decanter, where the liquid separates

into an aqueous phase and an organic phase. The aqueous phase is then fed back to the aqueous column or fermenter, and the organic phase is sent to the second column, where purified *n*-butanol is removed from the bottom.

Table 2.4: Compositions of *n*-butanol + water systems relevant to distillation and product recovery

System	*n*-Butanol (wt%)	Water (wt%)	Temperature (°C)	Reference
Azeotrope	55.5	44.5	92.5	Rumble, 2018
Solubility Limit				
Aqueous Phase	7.3	92.7	25.0	Butler, 1933
Organic Phase	79.7	20.3	25.0	Butler, 1933

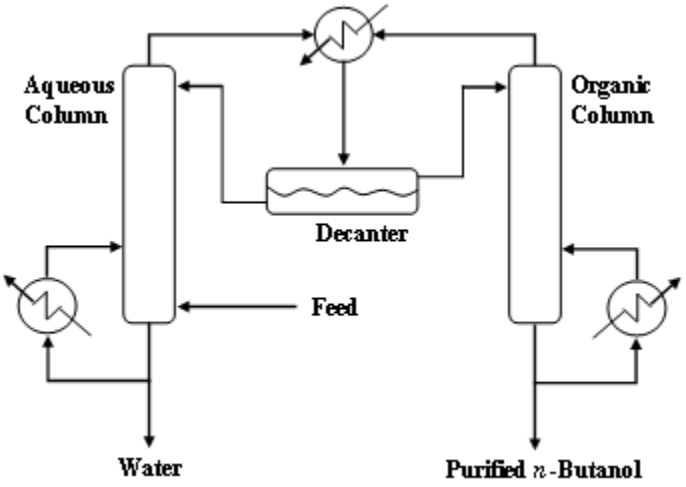

Figure 2.1: Flow of *n*-butanol purification process by distillation

In the traditional recovery of products from an ABE fermentation broth, ethanol and acetone are first removed from the stream by distillation before flowing towards the two-column *n*-butanol distillation system, as described by Roffler et al. (1987a). As the concentration of *n*-butanol in ABE fermentation broth is dilute, less than 2 wt% maximum, it is necessary to use the aqueous column to remove water from the feed to achieve phase separation in the decanter. Stripping water from *n*-butanol in the aqueous distillation column, however, is an expensive and energy intensive process, and therefore improvement to this stage of the *n*-butanol distillation

process has been investigated using ISPR technology (Roffler et al., 1987a). Through ISPR, including TPPB systems, gas stripping, and permeation membranes, *n*-butanol can be concentrated from the aqueous fermentation broth to be above its solubility limit, which can be removed and condensed, then fed directly to the decanter. This method may eliminate the need for the aqueous distillation column, as the aqueous phase of the decanter can be sent back to the bioreactor or contacted again with the extracting agent to concentrate *n*-butanol.

In addition, there is a relation between energy requirements and *n*-butanol concentration in the distillation process, in which as the feed concentration to the first column or decanter increases, energy requirements and subsequent expenses, decrease (Matsumura et al., 1988). Therefore, it is beneficial to input a feed that is as highly concentrated with *n*-butanol as possible, which relies on selectivity of the extractant for ISPR.

2.7 Recent Investigation of PILs as Extractants in Ethanol and ABE Fermentations

As PILs are highly absorbent materials, with impressive partitioning capabilities for desirable biofuel fermentation products, while circumventing previous toxicity issues, investigation into these materials is a potential step forward in biofuel ISPR technologies (Dafoe & Daugulis, 2014; Bacon et al., 2016; Bacon et al., 2017). Accordingly, Bacon et al. (2017) undertook the development and testing of poly(vinyldodecylimidazolium bromide) or P(VC_{12}ImBr), the chemical structure of which is seen in Figure 2.2, an imidazolium-based, semi-crystalline absorbent polymer synthesized through the polymerization of ionic liquid monomer 1-vinyl-3-dodecylimidazolium bromide, which produced promising results for affinity and selectivity for several fermentation products.

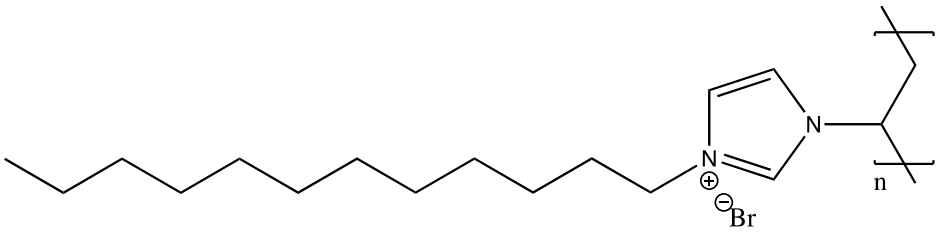

Figure 2.2: Chemical structure of P(VC_{12}ImBr)

Most notable in the work by Bacon et al. (2017) was the *n*-butanol partition coefficient and *n*-butanol/water selectivity, which were found to be 6.9 and 56, respectively, as seen in Table 2.5. Compared to oleyl alcohol, the PC of P(VC_{12}ImBr) is almost double, however the selectivity is much lower (Bacon et al., 2017). Alongside *n*-butanol absorption, P(VC_{12}ImBr) demonstrated encouraging results with other biofuel fermentation products, and these promising outcomes show the potential of P(VC_{12}ImBr) as an extractive phase in a TPPB system, whose sequestering abilities may lead to increased final product concentration and volumetric productivity in a fermentation, and aid in the ease of product recovery for downstream processing. Because of the noteworthy PC and selectivity of P(VC_{12}ImBr) for *n*-butanol as opposed to ethanol, along with benefits as a superior biofuel, there is sparked interest in its characterization and application for ABE fermentation process and *n*-butanol recovery (Bacon et al., 2017).

Table 2.5: Summary of previously found sorption capabilities of extractants for fermentation products

Molecule	Initial Solute Concentration (wt%)	P(VC_{12}ImBr)		Oleyl Alcohol	
		PC	$\alpha_{i/w}$	PC	$\alpha_{i/w}$
n-Butanol	1	6.9	56	3.6	180
Iso-butanol	1	5.6	40	2.7	135
Ethanol	1	1.1	7	0.3	24
Acetone	0.5	0.7	5		
Water	100	0.14	-		

Note: PC and selectivity values are from Bacon et al. (2017).

2.8 Scope of Thesis

The requirements for reducing carbon emissions have led to the investigation of biofuels as sustainable energy sources. Previous literature has consistently demonstrated toxicity and end-product inhibition occurring in biofuel fermentation processes, and as there is an increased demand for ethanol and *n*-butanol as renewable transportation energy sources, this work intended to improve biofuel production, with an emphasis on *n*-butanol as it has greater potential as a biofuel. The improvement of these fermentation processes is explored through the synthesis and investigation of P(VC_{12}ImBr) to sequester target molecules through ISPR, in an attempt to increase final product concentrations, volumetric productivities, and product recovery. Testing first focused on the characterization of P(VC_{12}ImBr), confirming the PC and selectivity values for the target molecules in question, along with determining other features such as density, melting and glass transition temperatures, diffusivity, and biocompatibility with *S. cerevisiae* and *C. acetobutylicum*. Next, ethanol and ABE fermentations were performed with P(VC_{12}ImBr) to sequester the target molecules in question, with improvements to final product concentrations and volumetric productivity only for the ABE fermentation. Finally, the removal of a concentrated *n*-butanol solution from P(VC_{12}ImBr) was achieved, and its impact on the *n*-butanol distillation process was considered.

2.9 References

Amsden, B.G., Bochanysz, J., & Daugulis, A.J. (2003). Degradation of xenobiotics in a partitioning bioreactor in which the partitioning phase is a polymer. *Biotechnology and Bioengineering, 84*(4), 399-405.

Antoni, D., Zverlov, V. V., & Schwarz, W. H. (2007). Biofuels from microbes. *Applied Microbiology and Biotechnology*, *77*(1), 23–35.

Atsumi, S., Hanai, T., & Liao, J.C. (2008). Non-fermentative pathways for synthesis of branched-chain higher alcohols as biofuels. *Nature, 451*(7174), 86-89.

Bacon, S.L., Peterson, E.C., Daugulis, A.J., & Parent, J.S. (2015). Selecting polymers for two-phase partitioning bioreactors (TPPBs): Consideration of thermodynamic affinity, crystallinity, and glass transition temperature. *Biotechnology Progress, 31*(6), 1500-1507.

Bacon, S.L., Daugulis, A.J., & Parent, J.S. (2016). Isobutylene-rich imidazolium ionomers for use in two-phase partitioning bioreactors. *Green Chemistry, 18*(24), 6586-6595.

Bacon, S.L., Ross, R.J., Daugulis, A.J., & Parent, J.S. (2017). Imidazolium-based polyionic liquid absorbents for bioproduct recovery. *Green Chemistry, 19*(21), 5203-5213.

Bai, F. W., Anderson, W. A., & Moo-Young, M. (2008). Ethanol fermentation technologies from sugar and starch feedstocks. *Biotechnology Advances*, *26*(1), 89–105.

Barton, A.F.M. (Ed.). (1984). Solubility data series (Vol. 15). Oxford: Pergamon Press.

Barton, W. E., & Daugulis, A. (1992). Evaluation of solvents for extractive butanol fermentation with *Clostridium acetobutylicum* and the use of poly(propylene glycol) 1200. *Applied Microbiology and Biotechnology*, *36*(5), 632–639.

Bunn, C.W. (1955). The melting points of chain polymers. *Journal of Polymer Science Part A: General Papers, 16*(82), 323-343.

Butamax. (2018). The bio-isobutanol advantage. Retrieved from http://www.butamax.com/The-Bio-Isobutanol-Advantage/The-Bio-Isobutanol-Advantage.aspx

Butler, J.A.V., Thomson, D.W., & Maclennan, W.H. (1933). The free energy of the normal aliphatic alcohols in aqueous solution. Part I. The partial vapour pressures of aqueous solutions of methyl, n-propyl, and n-butyl alcohols. Part II. The solubilities of some normal aliphatic alcohols in water. Part III. The theory of binary solutions, and its application to aqueous-alcoholic solutions. *Journal of the Chemical Society,* 674-686.

Bruce, L.J., & Daugulis, A.J. (1991). Solvent selection strategies for extractive biocatalysis. *Biotechnology Progress, 7*(2), 116-124.

Cascon, H.R., Choudhari, S.K., Nisola, G.M., Vivas, E.L., Lee, D., & Chung, W. (2011). Partitioning of butanol and other fermentation broth components in phosphonium and ammonium-based ionic liquids and their toxicity to solventogenic clostridia. *Separation and Purification Technology, 78*(2), 164-174.

Collins, L. D., & Daugulis, A. J. (1996). Use of a two phase partitioning bioreactor for the biodegradation of phenol. *Biotechnology Techniques*, *10*(9), 643–648.

Dafoe, J. T., & Daugulis, A. J. (2014). In situ product removal in fermentation systems: Improved process performance and rational extractant selection. *Biotechnology Letters*, *36*(3), 443–460.

Dale, B. E. (2003). "Greening" the chemical industry: Research and development priorities for biobased industrial products. *Journal of Chemical Technology and Biotechnology*, *78*(10), 1093–1103.

Daugulis, A.J., Axford, D.B., Ciszek, B., & Malinowski, J.J. (1994). Continuous fermentation of high-strength glucose feeds to ethanol. *Biotechnology Letters*, *16*(6), 637-642.

Daugulis, A. J., & Milton, S. G. (2012). Two-phase partitioning bioreactors: the use of polymers for the in situ removal of ethanol. *Asia-Pacific Journal of Chemical Engineering*, *7*(3), 324–328.

Fairley, P. (2011). Next generation biofuels. *Nature*, *474*(7352), S2-S5.

Fam, H., & Daugulis, A.J. (2012). Substrate mass transport in two-phase partitioning bioreactors employing liquid and solid non-aqueous phases. *Bioprocess and Biosystems Engineering, 35*(8), 1367-1374.

Gevo. (2018). Isobutanol blendstocks. Retrieved from https://gevo.com/isobutanol-blendstocks/

González-Peñas, H., Lu-Chau, T.A., Moreira, M.T., & Lema, J.M. (2014). Solvent screening methodology for in situ ABE extractive fermentation. *Applied Microbiology and Biotechnology, 98*(13), 5915-5924.

Hatti-Kaul, R., Törnvall, U., Gustafsson, L., & Börjesson, P. (2007). Industrial biotechnology for the production of bio-based chemicals - a cradle-to-grave perspective. *Trends in Biotechnology*, *25*(3), 119–124.

Huang, H., Ramaswamy, S., & Liu, Y. (2014). Separation and purification of biobutanol during bioconversion of biomass. *Separation and Purification Technology, 132*(20), 513-540.

Jiménez-Bonilla, P., & Wang, Y. (2018). *In situ* biobutanol recovery from clostridial fermentations: a critical review. *Critical Reviews in Biotechnology, 38*(3), 469-482.

Jin, C., Yao, M., Liu, H., Lee, C. F. F., & Ji, J. (2011). Progress in the production and application of n-butanol as a biofuel. *Renewable and Sustainable Energy Reviews*, *15*(8), 4080–4106.

Jones, T. D., Havard, J. M., & Daugulis, A. J. (1993). Ethanol production from lactose by extractive fermentation, *15*(8), 871–876.

Jones, D. T., & Woods, D. R. (1986). Acetone-butanol fermentation revisited. *Microbiological Reviews*, *50*(4), 484–524.

Kamm, B., & Kamm, M. (2004). Principles of biorefineries. *Applied Microbiology and Biotechnology*, *64*(2), 137–145.

Kollerup, F., & Daugulis, A. J. (1985). A mathematical model for ethanol production by extractive fermentation in a continuous stirred tank fermentor. *Biotechnology and Bioengineering*, *27*(1), 1335–1346.

Kujawska, A., Kujawski, J., Bryjak, M., & Kujawski, W. (2015). ABE fermentation products recovery methods - A review. *Renewable and Sustainable Energy Reviews*, *48*, 648–661.

Kumar, S., Singh, N., & Prasad, R., (2010). Anhydrous ethanol: A renewable source of energy. *Renewable and Sustainable Energy Reviews, 14*(7), 1830-1844.

Lin, Y., & Tanaka, S. (2006). Ethanol fermentation from biomass resources: Current state and prospects. *Applied Microbiology and Biotechnology*, *69*(6), 627–642.

Linden, J.C., Moreira, A.R., & Lenz, T.G. (1985). Acetone and Butanol. In Moo-Young (Ed.), *Comprehensive Biotechnology v.3* (915-929). Willowdale, ON: Pergamon Press.

Luyben, W.L. (2008). Control of the heterogeneous azeotropic *n*-butanol/water distillation system. *Energy & Fuels, 22*(6), 4249-4258.

Macleod, C.T., & Daugulis, A.J. (2003). Biodegradation of polycyclic aromatic hydrocarbons in a two-phase partitioning bioreactor in the presence of a bioavailable solvent. *Applied Microbiology and Biotechnology, 62*(2-3), 291-296

Mao, S., Hua, B., Wang, N., Hu, X., Ge, Z., Li, Y., … Lu, F. (2013). 11α hydroxylation of 16α, 17-epoxyprogesterone in biphasic ionic liquid/water system by Aspergillus ochraceus. *Journal of Chemical Technology and Biotechnology*, *88*(2), 287–292.

Maiorella, B.L. (1985). Ethanol. In Moo-Young (Ed.), *Comprehensive Biotechnology v.3* (862-909). Willowdale, ON: Pergamon Press.

McGovern, P. E., Zhang, J., Tang, J., Zhang, Z., Hall, G. R., Moreau, R. A., … Wang, C. (2004). Fermented beverages of pre- and proto-historic China. *Proceedings of the National Academy of Sciences of the United States of America*, *101*(51), 17593–8.

Minier, M., & Goma, G. (1982). Ethanol Production by Extractive Fermentation. *Biotechnology and Bioengineering, 24*(7), 1565-1579.

Mirata, M.A., Heerd, D., & Schrader, J. (2009). Integrated bioprocess for the oxidation of limonene to perillic acid with *Pseudomonas putida* DSM 12264. *Process Biochemistry*, *44*(7), 764-771.

National Research Council. (2000). *Biobased Industrial Products: Priorities for Research and Commercialization*. Washington, DC: National Academy Press.

Natural Resources Canada. (2016). Ethanol. Retrieved from http://www.nrcan.gc.ca/energy/alternative-fuels/fuel-facts/ethanol/3493#a7

Naik, S.N., Goud, V.V., Rout, P.K., & Dalai, A.K. (2010). Production of first and second generation biofuels: A comprehensive review. *Renewable and Sustainable Energy Reviews, 14*(2), 578-597.

Najafpour, G., Younesi, H., & Ku Ismail, K. S. (2004). Ethanol fermentation in an immobilized cell reactor using Saccharomyces cerevisiae. *Bioresource Technology*, *92*(3), 251–260.

Ndaba, B., Chiyanzu, I., & Marx, S. (2015). *n*-Butanol derived from biochemical and chemical routes: A review. *Biotechnology Reports, 8*, 1-9.

Nielsen, D. R., & Prather, K. J. (2009). *In situ* product recovery of *n*-butanol using polymeric resins. *Biotechnology and Bioengineering*, *102*(3), 811–821.

Oudshoorn, A., van der Wielen, L.A.M., & Straathof, A.J.J. (2009). Assessment of options for selective 1-butanol recovery from aqueous solution. *Industrial & Engineering Chemistry Research, 48*(15), 7325-7336.

Outram, V., Lalander, C., Lee, J.G.M, Davies, E.T., Harvey, A.P. (2017). Applied in situ product recovery in ABE fermentation. *Biotechnology Progress, 33*(3), 563-579.

Parent, J.S., Capela, M, Dafoe, J.T., & Daugulis, A.J. (2012). First principles approach to identifying polymers for use in two-phase partitioning bioreactors. *Journal of Chemical Technology and Biotechnology, 87*(8), 1059-1065.

Pittman, M. J., Bodley, M. W., & Daugulis, A. J. (2015). Mass transfer considerations in solid-liquid two-phase partitioning bioreactors: a polymer selection guide. *Journal of Chemical Technology & Biotechnology*, *90*(8), 1391–1399.

Poleo, E. E., & Daugulis, A. J. (2014). A comparison of three first principles methods for predicting solute-polymer affinity, and the simultaneous biodegradation of phenol and butyl acetate in a two-phase partitioning bioreactor. *Journal of Chemical Technology and Biotechnology*, *89*(1), 88–96.

Qureshi, N., & Ezeji, T.C. (2008). Butanol, 'a superior biofuel' production from agricultural residues (renewable biomass): recent progress in technology. Biofuels, Bioproducts and Biorefining, *2*(4), 319-330.

Qureshi, N., Hughes, S., Maddox, I.S., & Cotta, M.A. (2005). Energy-efficient recovery of butanol from model solutions and fermentation broth by adsorption. *Bioprocess and Biosystems Engineering, 27*(4), 215-222.

Ragauskas, A. J., Williams, C. K., Davison, B. H., Britovsek, G., Cairney, J., Eckert, C. A., … Tschaplinski, T. (2006). The path forward for biofuels and biomaterials. *Science (New York, N.Y.)*, *311*(5760), 484–9.

Roffler, S.R., Blanch, H.W., & Wilke, C.R. (1984). *In situ* recovery of fermentation products. *Trends in Biotechnology, 2*(5), 129-136.

Roffler, S.R., Blanch, H.W., & Wilke, C.R. (1987a). Extractive fermentation of acetone and butanol: process design and economic evaluation. *Biotechnology Progress, 3*(3), 131-140.

Roffler, S.R., Blanch, H.W., & Wilke, C.R. (1987b). *In-situ* recovery of butanol during fermentation. Part 1: Batch extractive fermentation. *Bioprocess Engineering, 2*(1), 1-12.

Roffler, S.R., Blanch, H.W., & Wilke, C.R. (1988). In situ extractive fermentation of acetone and butanol. *Biotechnology and Bioengineering, 31*(2), 135-143.

Rumble, J.R. (Ed.). (2018). *CRC Handbook of Chemistry and Physics, 99th Edition*. CRC Press.

Sonego, J.L.S., Lemos, D.A., Cruz, A.J.G., & Badino, A.C. (2018). Optimization of fed-batch fermentation with in situ ethanol removal by CO2 Stripping. *Energy & Fuels, 32*(1), 954-960.

Staggs, K. W., & Nielsen, D. R. (2015). Improving n-butanol production in batch and semi-continuous processes through integrated product recovery. *Process Biochemistry*, *50*(10), 1487–1498.

Tao, L., Tan, E.C.D., McCormick, R., Zhang, M., Aden, A., He, X., & Zigler, B.T. (2014). Techno-economic analysis and life-cycle assessment of cellulosic isobutanol and comparison with cellulosic ethanol and *n*-butanol. *Biofuels, Bioproducts and Biorefining, 8*(1), 30-48.

United States Environmental Protection Agency. (2018). Renewable Fuel Standard Program. Retrieved from https://www.epa.gov/renewable-fuel-standard-program

Van Hecke, W., Kaur, G., & De Wever, H. (2014). Advances in *in-situ* product recovery (ISPR) in whole cell biotechnology during the last decade. *Biotechnology Advances, 32*(7), 1245-1255.

Vane, L.M. (2008). Separation technologies for the recovery and dehydration of alcohols from fermentation broths. *Biofuels, Bioproducts & Biorefining, 2*(6), 553-588.

Wang, P., Wang, Y., Liu, Y., Shi, H., & Su, Z. (2012). Novel in situ product removal technique for simultaneous production of propionic acid and vitamin B12 by expanded bed adsorption bioreactor. *Bioresource Technology*, *104*, 652–659.

Xue, C., Zhao, J. B., Chen, L. J., Bai, F. W., Yang, S. T., & Sun, J. X. (2014). Integrated butanol recovery for an advanced biofuel: Current state and prospects. *Applied Microbiology and Biotechnology*, *98*(8), 3463–3474.

Xue, C., Zhao, J., Lu, C., Yang, S. T., Bai, F., & Tang, I. C. (2012). High-titer *n*-butanol production by *Clostridium acetobutylicum* JB200 in fed-batch fermentation with intermittent gas stripping. *Biotechnology and Bioengineering*, *109*(11), 2746–2756.

Yang, X., Tsai, G., & Tsao, G.T. (1994). Enhancement of in situ adsorption on the acetone-butanol fermentation by *Clostridium acetobutylicum. Separations Technology, 4*(2), 81-92.

Yuan, J., & Antonietti, M. (2011). Poly(ionic liquid)s: polymers expanding classical property profiles. *Polymer, 52*(7), 1469-1482.

Zhao, N., Bai, Y., Liu, C., Xu, J., & Bai, F. (2014). Flocculating *Zymomonas mobilis* is a promising host to be engineering for fuel ethanol production from lignocellulosic biomass. *Biotechnology Journal, 9*(3), 362-371.

Chapter 3

Materials and Methods

3.1 Chemicals

All chemical reagents were purchased from either Sigma-Aldrich (Oakville, Ontario) or Fisher Scientific (Ottawa, Ontario), at the highest purity grade available and were used as received. All medium components were purchased from either Sigma-Aldrich (Oakville, ON) or Fisher Scientific (Ottawa, Ontario). Type I ultrapure water (18.2 MΩ cm at 25°C) or HPLC grade water obtained from Fisher Scientific (Ottawa, Ontario) were used throughout all experiments and analytical procedures.

3.2 Synthesis of P(VC_{12}ImBr)

The ionic liquid monomer [VC_{12}Im][Br] was prepared as previously described by Bacon et al. (2017) and characterized by ^{1}H-NMR. Solution polymerization of the IL monomer to solid PIL P(VC_{12}ImBr) with 2,2′-azobis(2-methylpropionitrile) (AIBN) initiator (toluene/ethanol) occurred as previously described (Bacon et al., 2017) and was characterized by ^{1}H-NMR.

To form polymer pieces, P(VC_{12}ImBr) was ground to a fine powder with a mortar and pestle and added to 20% (v/v) ethanol-water solution in a 1 g per 10 mL ratio. The plasticized material was then flattened by hydraulic press (Wabash, USA) for 2 mins at 10000 lb and 30°C, creating a sheet of 2 mm thickness, and was cut by hand into rectangular pieces that were approximately 9 mm by 6 mm. The formed polymer pieces were then dried in a 60°C oven until the mass remained unchanged to remove excess ethanol, the final form of which can be seen in Figure 3.1.

Figure 3.1: Pieces of P(VC_{12}ImBr) that were synthesized and formed for use in this work next to a dime for size reference.

3.3 Microorganisms and Media Formulations

Saccharomyces cerevisiae was obtained from Alltech (Nicholasville, Kentucky) and cultivated in a medium based on that of Doran and Bailey (1986), listed in Table 3.1. *Clostridium acetobutylicum* ATCC 824 was obtained from Cedarlane (Burlington, Ontario) and was grown in medium prepared according to Barton & Daugulis (1992), detailed in Table 3.2, that had already been sparged with nitrogen to ensure anaerobic conditions. All medium solutions used were autoclaved separately prior to inoculation.

Table 3.1: *S. cerevisiae* medium composition

Solution	Component	S.C. Medium A (g/L)	S.C. Medium B (g/L)
I	**Glucose**	10	200
II	**Yeast Extract**	2	2
	KH_2PO_4	5	5
	$(NH_4)_2SO_4$	2	2
	$MgSO_4 \bullet 7H_2O$	0.4	0.4
	$CaCl_2$	0.1	0.1

Note: S.C. Medium A was used for inoculation and biocompatibility testing, and S.C. Medium B for fermentations.

Table 3.2: *C. acetobutylicum* medium composition

Solution	Component	C.A. Medium A (g/L)	C.A. Medium B (g/L)
I	**Glucose**	10	70
II	**Tryptone**	4.0	4.7
	Yeast extract	5.0	1.2
III	**Ammonium acetate**	2.3	2.8
	KH_2PO_4	0.5	0.58
	K_2HPO_4	0.5	0.58
IV	**$MgSO_4 \cdot 7H_2O$**	0.2	0.23
	$MnSO_4 \cdot 7H_2O$	0.01	0.012
	$FeSO_4 \cdot 7H_2O$	0.01	0.012
V	***p*-Aminobenzoic acid**	0.001	0.0012
	Biotin	0.00001	0.000012

Note: C.A. Medium A was used for inoculation, biocompatibility testing, and ion experiments, and C.A. Medium B for fermentations.

3.4 Characterization of P(VC_{12}ImBr) for *in-situ* Product Removal Applications

The following section describes the characterization of P(VC_{12}ImBr) as an ISPR extractant. The characterization is focused on the production of *n*-butanol, including its fermentation process and subsequent recovery, as P(VC_{12}ImBr) is a superior biofuel.

3.4.1 Partition Coefficient and Selectivity Experiments for P(VC_{12}ImBr)

Pieces of P(VC_{12}ImBr) were initially soaked in water for at least 24 hours prior to partition coefficient and selectivity experiments, as it had been previously determined that plasticization by water can improve solute absorption (Bacon et al., 2015). The water-soaked pieces of P(VC_{12}ImBr) were then lightly pat dried with paper towel and weighed for experiments and mass balance calculations.

Aqueous solutions (10 mL) of known solute concentrations were prepared for *n*-butanol (1 wt%), ethanol (1 wt%), or acetone (0.5 wt%), and were added to scintillation vials, along with 5% (w/v) P(VC_{12}ImBr). The vials were then sealed with a foil lined cap and incubated at 30°C and 180 rpm for 24 hours. Once equilibrated, the pieces of P(VC_{12}ImBr) in each sample were lightly

pat dried with a paper towel and weighed, then dried in an oven at 60°C until the polymer mass remained unchanged, which signified that liquid had been fully desorbed, and the weight was recorded for determining the partition coefficient and selectivity.

To determine water and solute uptake by P(VC_{12}ImBr), mass balances were performed, using the mass of the water-soaked polymer, the mass of the polymer at equilibrium with the aqueous solution, the mass of the dry polymer, and the solute concentrations of the aqueous sample before and after equilibrium had been reached. From these mass balance calculations, the aqueous and polymer weight fractions (w_i^{aq} and w_i^p) of triplicate samples were found, from which the mean partition coefficient for each solute (PC_i) was determined.

$$PC_i = \frac{w_i^e}{w_i^{aq}} \quad \textbf{(3.1)}$$

The solute/water selectivity of P(VC_{12}ImBr) was then found after the PC determination.

$$\alpha_{i/w} = \frac{PC_i}{PC_w} \quad \textbf{(3.2)}$$

Example calculations for determining the partition coefficient and selectivity are in Appendix B.

3.4.2 Density

The density of P(VC_{12}ImBr) was measured with a Mirage MD-200S electronic densimeter based on the water displacement method (Alfa Mirage, 2014). Triplicate samples of dry P(VC_{12}ImBr) of approximately 0.5 g each were placed on the densimeter, which gave a reading of the density.

3.4.3 Differential Scanning Calorimetry (DSC) Analysis

Differential scanning calorimetry was used to measure temperature effects, including finding the melting temperature (T_m) and glass transition temperature (T_g), of P(VC_{12}ImBr) in an unplasticized state. To ensure P(VC_{12}ImBr) was not plasticized by any solvent prior to analysis, the material was vacuum dried overnight at 60°C. A DSC Q100 (Texas Instruments) apparatus operating at a heating rate of 5°C/min under nitrogen purge of 50 mL/min measured the melting

endotherm of 0.5 g sample of P(VC_{12}ImBr) over a range of -60°C to 210°C, of which the second heating scan was used to represent the data.

3.4.4 Rate of Uptake and Diffusivity of P(VC_{12}ImBr)

The rate of uptake and diffusivity of *n*-butanol into P(VC_{12}ImBr) were determined experimentally using a 1-L working volume reactor (Bioflo I, New Brunswick Scientific, USA), fitted with a six-blade Rushton impeller operating at 300 rpm and 22.5°C. The aqueous phase had an initial concentration of 2 wt% *n*-butanol with a solid phase mass fraction of 5% (w/v) P(VC_{12}ImBr) pieces that had been plasticized in water and then pat dried with a paper towel, which were added at time zero. Aqueous samples were taken every 5 minutes until the 30-minute mark, after which the sampling frequency was decreased until equilibrium was assumed to be reached after 8 hours. The samples were measured using gas chromatography, as described below, to determine the level of *n*-butanol in the aqueous solution at each time point.

The fractional uptake of n-butanol by P(VC_{12}ImBr) time course data, along with the average radius of the polymer (0.0027 mm), were used to find diffusivity through the Crank Equation (Crank, 1975), in which a least squares regression analysis was undertaken to fit the experimental data and develop model for the specific system, as previously described (Amsden et al., 2003; Pittman et al., 2015).

3.4.5 Biocompatibility

S.C. Medium A (50 mL) was freshly prepared and added to six 125 mL Erlenmeyer flasks with foam stoppers. P(VC_{12}ImBr) that had been soaked in water for 24 hours was pat dried with a paper towel to remove excess liquid, then weighed (approximately 2.5 g each) and sterilized separately from the medium. The water-soaked polymer was then added aseptically to triplicate flasks, and 2 mL each of *S. cerevisiae* -80°C glycerol stock culture was added to all six flasks. Flasks were then incubated at 30°C and 180 rpm for 24 hours.

For *C. acetobutylicum* biocompatibility, P(VC_{12}ImBr) (2.5 g) was added each to three empty 125 mL serum bottles, then sparged with N_2 to ensure anaerobic conditions and sterilized. C.A. Medium A (50 mL) was prepared anaerobically and added to six 125 mL serum bottles, three of which contained the samples of P(VC_{12}ImBr). Inoculation was by the addition of -80°C glycerol stock culture of *C. acetobutylicum* to each of the six serum bottles, followed by incubation at 37°C and 180 rpm for 24 hours.

Following 24 hours of incubation, the biomass and residual glucose were determined as described below in Section 3.8. Biocompatibility was determined by comparing biomass growth and residual glucose levels of the samples with P(VC_{12}ImBr) to the control samples without polymer.

3.4.6 Ion Exchange Experiments

Testing was performed to determine if there was ion exchange occurring between bromide ions in P(VC_{12}ImBr) and sulphate and phosphate ions in the ABE fermentation medium. The possible exchange and therefore removal of these medium anions could potentially decrease cell growth and also compromise the effectiveness of the polymer for sequestration of target molecules. Experiments were run in triplicate using 10 mL of C.A. Medium B, prepared as listed in Table 3.2, which was added to scintillation vials with 5% (w/v) P(VC_{12}ImBr). Samples were incubated for 24 hours at 37°C and 180 rpm to reach equilibrium. Following incubation, the aqueous samples were filtered through a sterile 0.2 μm syringe filter, then sent to Queen's Analytical Services Unit (Kingston, Ontario, Canada) for ion detection, which was used in mass balance calculations to determine the uptake of ions from fermentation medium with P(VC_{12}ImBr).

3.4.7 Analyte Competition

PC tests were performed to confirm that the PC and selectivity of P(VC_{12}ImBr) for *n*-butanol were maintained when interacting with constituents present in an ABE fermentation,

including medium components and fermentation products. This experiment was done to confirm that possible anion exchange between P(VC_{12}ImBr) and medium nutrients do not influence the polymer's effectiveness to extract target molecules. Experiments were performed in triplicate, in which 5% (w/v) of P(VC_{12}ImBr), which had been plasticized in water then pat dried with a paper towel, was added to a 50 mL solution containing the approximate maximum solvent and acid product concentrations present in an ABE fermentation (1 wt% *n*-butanol, 0.5 wt% acetone, 0.2 wt% ethanol, 0.5 wt% butyric acid, and 0.5 wt% acetic acid), and the constituents of C.A. Medium B as listed in Table 3.2. Following sample incubation for 24 hours at 37°C and 180 rpm, the aqueous phase was filtered for solvent detection to determine the PC and selectivity of P(VC_{12}ImBr) for *n*-butanol, along with the PCs for ethanol and acetone.

3.5 Biofuel Fermentations

3.5.1 Ethanol Fermentation

A control ethanol fermentation was conducted in a 5 L BioFlo III Bioreactor (New Brunswick Scientific, USA) with a working volume of 3 L of medium, which was autoclaved prior to inoculation. The composition of the fermentation medium is listed in Table 3.1 as S.C. Medium B, in which solution I and II were prepared and autoclaved separately to prevent unwanted reactions (Mermelstein et al., 1994; Wang, 1995). The fermentation was initiated by the addition of 10% (v/v) inoculum of 50 mL aliquots in six 125 mL Erlenmeyer flasks that had been incubated for 24 hours prior with the addition of a 2 mL -80°C glycerol stock culture to SC. Medium A. The bioreactor was maintained at 30°C and agitated at 300 rpm for 50 hours. Throughout the fermentation the pH of the medium was adjusted to 4.5 by automatic addition of a 3 M KOH solution.

The ISPR ethanol fermentation was carried out under the same conditions as the control fermentation, up until the 18-hour mark prior to the anticipated inhibitory aqueous ethanol concentration, at which point the bioreactor contents were circulated through a column packed with

P(VC_{12}ImBr) via a peristaltic pump. The flow of fermentation broth through the 500 mL glass column was at 30 mL/min, which contained approximately 150 g (dry weight) or 5% (w/v) of P(VC_{12}ImBr) polymer and circulated continuously back to the reactor until completion of the fermentation at 50 hours.

For both control and ISPR fermentations, aqueous samples were taken in conjunction with expected ethanol fermentation kinetics to determine cell growth, ethanol production, and glucose consumption. Following immediate cell density measurements, the remaining sample was centrifuged in capped Eppendorf tubes at 3600 rpm for 30 minutes at 10°C. The supernatant was then decanted, filtered through a sterile 0.2 μm syringe filter, and diluted accordingly for product and substrate concentration analysis.

3.5.2 ABE Fermentation

C. acetobutylicum ATCC 824 was grown in C.A. Medium A at 37°C and 180 rpm in airtight serum bottles, inoculated with of 2 mL of -80°C glycerol stock culture. After 24 hours, 10% (v/v) of the culture was propagated into six serum bottles containing fresh C.A. Medium A and grown for an additional 12 hours to reach the exponential growth phase for inoculation. The control ABE fermentation was conducted in a 5 L BioFlo III Bioreactor with a working volume of 3 L of C.A. Medium B, which was autoclaved prior to inoculation. The medium composition is detailed in Table 3.2, where each solution was prepared separately to circumvent unwanted reactions in sterilization procedures (Mermelstein et al., 1994). Solutions I-III were autoclaved and solutions IV and V were sterilized through a 0.2 μm aseptic syringe filter before added to the bioreactor (Li et al., 2010; Mermelstein et al., 1994). After sterilization of the bioreactor and medium components, filtered N_2 gas was sparged through the reactor prior to inoculation to create an oxygen-free environment until anaerobic cell growth was observed (Yang et al., 1994). The fermentation was initiated by the anaerobic addition of 10% v/v inoculum to the bioreactor, which was set at 37°C and agitated continuously at 150 rpm for 50 hours with uncontrolled pH.

The ISPR ABE fermentation was carried out under the same conditions as the control fermentation, up until the 10-hour mark, prior to anticipated inhibitory *n*-butanol concentrations, at which point the bioreactor contents were circulated through a column packed with P(VC_{12}ImBr) via a peristaltic pump. The flow of fermentation broth through the 500 mL glass column was at 50 mL/min, which contained approximately 150 g (dry weight) or 5% (w/v) of P(VC_{12}ImBr) polymer and circulated continuously back to the reactor upon conclusion of the fermentation at 50 hours.

For both control and ISPR fermentations, aqueous samples were taken in conjunction with expected ABE fermentation kinetics to determine cell growth, solvent and acid production, and glucose consumption. Following immediate cell density measurements, the remaining sample was centrifuged in capped Eppendorf tubes at 10000 rpm for 10 minutes at 10°C. The supernatant was then decanted, filtered through a sterile 0.2 μm syringe filter, and diluted accordingly for product and substrate concentration analysis.

3.6 Ternary Phase Diagram

A ternary diagram was constructed to show the equilibrium behavior of the water + *n*-butanol + P(VC_{12}ImBr) system over a range of initial *n*-butanol concentrations. This ternary phase information was used to determine if P(VC_{12}ImBr) can absorb concentrations of *n*-butanol above its solubility limit in water. Samples containing 10 mL of *n*-butanol solution were added to scintillation vials with 5% (w/v) P(VC_{12}ImBr) that had been plasticized in water then pat dried with a paper towel. The initial *n*-butanol content ranged from 1 wt% to 6 wt% of the entire system. Samples were then incubated for 24 hours at 37°C and 180 rpm to reach equilibrium, then filtered for *n*-butanol detection. The polymer pieces in each equilibrated sample were lightly pat dried with a paper towel and then weighed. A mass balance was then performed to determine the composition of the aqueous and P(VC_{12}ImBr) phases at equilibrium.

3.7 Recovery of *n*-Butanol from P(VC_{12}ImBr)

Thermal desorption experiments were performed to recover *n*-butanol from P(VC_{12}ImBr). Water-soaked P(VC_{12}ImBr) (30 g) was weighed and added to an Erlenmeyer flask containing 100 mL of a 2 wt% *n*-butanol concentration solution and incubated for 48 hours at 37°C and 180 rpm. Once equilibrated, an aqueous sample was taken from the flask to determine the remaining *n*-butanol content, and the polymer was lightly pat dried with a paper towel to remove excess liquid and weighed, then placed in a container for thermal desorption. A mass balance was then performed to determine the amount of *n*-butanol and water in the polymer.

The thermal desorption setup consisted of two 125 mL airtight straight sided round bottles that were connected by tubing through each lid. One container contained the equilibrated polymer and was placed in a retrofitted microwave oven (Kenmore, USA), with the tubing connection leading out through the side of the microwave to the other container, which was submerged in ice chips. The microwave was run for 25 minutes on 50% power, which removed the liquid from P(VC_{12}ImBr), and the condensed aqueous *n*-butanol solution was collected in the chilled container, from which a sample was taken to determine the amount of *n*-butanol that was recovered from the polymer.

3.8 Analytical Methods

3.8.1 Product and Substrate Concentrations

Aqueous samples of solute concentration were taken in triplicate for each experiment. *n*-Butanol, ethanol, and acetone concentration was analyzed by gas chromatography, using a Varian 450-GC gas chromatographer with a CP-8410 AutoInjector, Restek RTX 502.2 capillary column, and FID detector. Acetic acid and butyric acid concentration were determined through HPLC (Varian Prostar) with a UV-Vis detector (PS 325, Varian Prostar) operating at 220 nm, using a Varian Hi-Plex H column (300 x 7.7 mm) at 60°C with a 9 mM H_2SO_4 mobile phase at 0.4 mL/min. Glucose concentration was determined through HPLC (Varian Prostar) with a refractive index

detector (PS 356, Varian Prostar), using a Varian Hi-Plex H column (300 x 7.7 mm) at 60°C with a 9 mM H_2SO_4 mobile phase at 0.4 mL/min.

3.8.2 Optical Density

Cell growth was measured from samples in triplicate through optical density at 600 nm (OD_{600}) using a Biochrom Ultrospec 3000 UV/Visible Spectrophotometer and correlated with a previously determined cell dry weight (g/L) calibration curve shown in Appendix A. Samples were diluted with water to observe optical density in a linear range.

3.8.3 Ion Detection

In ion exchange experiments, the cation species concentration was measured by inductively coupled plasma-optical emission spectrometry (Varian Vista Pro-axial CCD spectrometer) combined with a CETAC ultrasonic nebulizer (U5000AT+), and the concentration of anion species was found by ion-chromatography (Dionex ICS-3000).

3.9 References

Alfa Mirage. (2014). Electronic densimeter. Alfa Mirage Co., Ltd., Osaka, Japan.

Amsden, B.G., Bochanysz, J., & Daugulis, A.J. (2003). Degradation of xenobiotics in a partitioning bioreactor in which the partitioning phase is a polymer. *Biotechnology and Bioengineering, 84*(4), 399-405.

Bacon, S.L., Ross, R.J., Daugulis, A.J., & Parent, J.S. (2017). Imidazolium-based polyionic liquid absorbents for bioproduct recovery. *Green Chemistry, 19*(21), 5203-5213.

Barton, W. E., & Daugulis, A. (1992). Evaluation of solvents for extractive butanol fermentation with *Clostridium acetobutylicum* and the use of poly(propylene glycol) 1200. *Applied Microbiology and Biotechnology*, *36*(5), 632–639.

Crank, J. (1975). *The mathematics of diffusion*. New York: Academic Press.

Doran, P.M., & Bailey, J.E. (1986). Effects of immobilization on growth, fermentation properties, and macromolecular composition of *Saccharomyces cerevisiae* attached to gelatin. *Biotechnology and Bioengineering, 28*(1), 73-87.

Li, S. Srivastava, R., Suib, S.L., Li, Y., & Parnas, R.S. (2010). Performance of batch, fed-batch, and continuous A-B-E fermentation with pH-control. *Bioresource Technology, 102*(5), 4241-4250.

Mermelstein, L.D., Welker, N.E., Petersen, D.J., Bennett, G.N., & Papoutsakis, E.T. (1994). Genetic and metabolic engineering of *Clostridium acetobutylicum* ATCC 824. *Recombinant DNA Technology II, 721*(1), 54-68

Pittman, M. J., Bodley, M. W., & Daugulis, A. J. (2015). Mass transfer considerations in solid-liquid two-phase partitioning bioreactors: a polymer selection guide. *Journal of Chemical Technology & Biotechnology*, *90*(8), 1391–1399.

Wang, X., & Hsiao, K. (1995). Sugar degradation during autoclaving: Effects of duration and solution volume on breakdown of glucose. Physiologia Plantarum, 94(3), 415-418.

Yang, X., Tsai, G., & Tsao, G.T. (1994). Enhancement of in situ adsorption on the acetone-butanol fermentation by *Clostridium acetobutylicum. Separations Technology, 4*(2), 81-92.

Chapter 4

Results and Discussion

4.1 Characterization of P(VC_{12}ImBr) for *in-situ* Product Removal Applications

The initial stages of this work involved characterizing P(VC_{12}ImBr) as an ISPR extractant for biofuel fermentation processes, with a focus on the production of *n*-butanol in an ABE fermentation.

4.1.1 Partition Coefficient and Selectivity

The PC and selectivity of a material are performance figures used to assess the ability of an absorbent to sequester a target molecule and to allow desorption of the solute without significant dilution by any water present. Accordingly, the PC and selectivity of P(VC_{12}ImBr) for *n*-butanol were found simultaneously through experiment in this work to be 6.5 and 46, respectively, as listed in Table 4.1. These values coincide with previously found P(VC_{12}ImBr) PC and selectivity values for *n*-butanol by Bacon et al. (2017), along with values for other desired fermentation products, demonstrating the consistency of this material as an extractant for TPPB applications.

The PC of P(VC_{12}ImBr) for *n*-butanol is among the highest for biocompatible extractants used for ABE ISPR, especially compared to commonly studied oleyl alcohol, which has a reported PC of around 3.7 (Barton & Daugulis, 1992; Malinowski & Daugulis, 1994). In addition, the PCs of P(VC_{12}ImBr) for ethanol and acetone surpass oleyl alcohol's reported PCs of 0.22 and 0.07 (Malinowski & Daugulis, 1994), respectively, which are target molecules in ethanol and ABE fermentations.

In Table 4.1, the selectivity of P(VC_{12}ImBr) shows that this material will preferentially take up *n*-butanol, relative to acetone and ethanol, due to its higher value, which is desired in an ABE fermentation, where toxicity to *C. acetobutylicum* occurs at *n*-butanol low concentrations. However, the selectivity of P(VC_{12}ImBr) for *n*-butanol is lower than that of oleyl alcohol, which is

around 180 (Matsumura et al., 1988), albeit does not necessarily mean it is more effective in a TPPB application for ABE fermentations, as its PC is lower. The higher selectivity of P(VC_{12}ImBr) for *n*-butanol as compared to other solutes also alludes to the idea that this material could absorb a highly concentrated *n*-butanol solution, which is important for subsequent recovery, as discussed in later sections.

Table 4.1: Summary and comparison of sorption capabilities for fermentation products by P(VC_{12}ImBr) found in this work

Molecule	PC	α
P(VC_{12}ImBr)		
n-Butanol	6.5 ± 0.4	46 ± 4
Ethanol	1.1 ± 0.4	7.2 ± 2
Acetone	1.3 ± 0.3	8.5 ± 2
Oleyl Alcohol		
n-Butanol	3.7	180
Ethanol	0.22	25
Acetone	0.07	n/a

Note: Error shows standard deviation from triplicate samples (n=3). Oleyl alcohol PC and α from experimental values by Matsumura et al. (1988), Barton & Daugulis (1992), and Malinowski & Daugulis (1994).

4.1.2 Density

The density of P(VC_{12}ImBr) was found to be 1.07 ± 0.015 g/cm^3, which is slightly lower than other polymers that have been used successfully as solid bead extractants in TPPB systems, as outlined in Table 4.2. Knowing the density is useful as it provides information regarding the volume of P(VC_{12}ImBr) required to keep products below their inhibitory levels in a bioreactor, as the mass fraction of polymer used for ISPR governs the amount of a target molecule absorbed. In addition, knowing the density is useful when considering how P(VC_{12}ImBr) might need to be handled physically in either a direct ISPR arrangement or in an external packed column, as well as during conveyance in desorption and reuse parts of an integrated process.

Table 4.2: Densities of solid materials as bead shape that have been used as secondary phases in TPPB systems

Material	Density (g/cm^3)	Reference
P(VC_{12}ImBr)	1.07	This Work
Silicone rubber	1.15	Littlejohns & Daugulis, 2008
Hytrel 8206	1.17	Pittman et al., 2015
Hytrel 3548	1.16	Pittman et al., 2015
Hytrel 5544	1.22	Pittman et al., 2015

4.1.3 Differential Scanning Calorimetry (DSC) Analysis

The DSC scan shown in Figure 4.1 provides the effects of temperature on P(VC_{12}ImBr), ranging from -60°C to 210°C, including its melting temperature (T_m) and glass transition temperature (T_g). The T_m of P(VC_{12}ImBr) was found to be -17°C, which is below the bioreactor operation temperature to allow for improved sorption (Bacon et al., 2015; Bacon et al., 2017). However, this sample of P(VC_{12}ImBr) does not display a visible T_g prior to 210°C, indicating that it is in an unabsorptive glassy state over this temperature range, which is not desirable for effective solute uptake (Bacon et al., 2014; Parent et al., 2012). However, in the case of a TPPB fermentation, P(VC_{12}ImBr) will become plasticized when in contact with water, which will lower

its T_g and allow for improved uptake of *n*-butanol (Bacon et al., 2015; Bacon et al., 2017). The T_g of P(VC_{12}ImBr) in a plasticized state was not found as it would be too broad to be displayed.

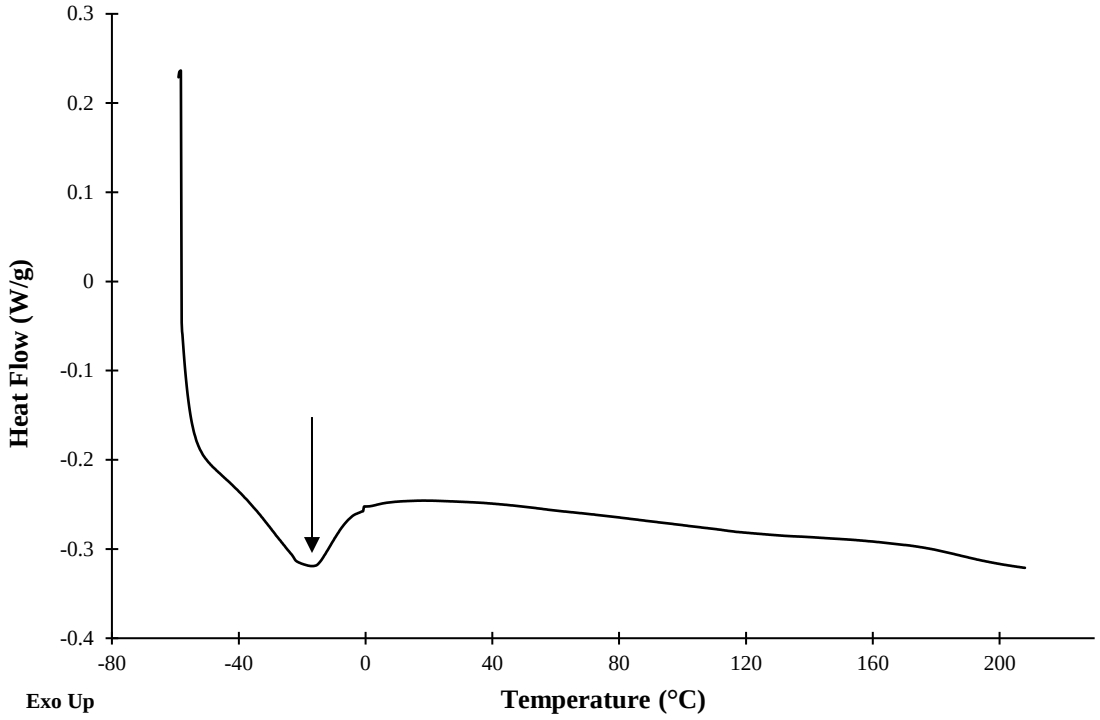

Figure 4.1: Second heating DSC scan of P(VC_{12}ImBr). The arrow marks the peak indicating the T_m of P(VC_{12}ImBr).

4.1.4 Rate of Uptake and Diffusivity of P(VC_{12}ImBr)

The diffusivity of *n*-butanol into P(VC_{12}ImBr) was determined to characterize its ability to reduce inhibitory levels of *n*-butanol at a rate required for an ABE fermentation. The experimental fractional uptake of *n*-butanol by P(VC_{12}ImBr), along with a fit of the model by the Crank Equation, is displayed in Figure 4.2. The experimental data show an initial rapid uptake of *n*-butanol by P(VC_{12}ImBr) in approximately 2 hours, reaching a state of equilibrium by the 7-hour mark. As almost 90% of *n*-butanol absorbed by P(VC_{12}ImBr) occurs in just over 3 hours, this rapid uptake is expected to sufficiently sequester *n*-butanol in an ABE batch fermentation by *C. acetobutylicum*, where exponential growth occurs over 10 hours to produce most of the *n*-butanol (Barton and

Daugulis, 1992). Therefore, if absorption by P(VC_{12}ImBr) begins prior to the accumulation of *n*-butanol at a toxic level in the fermentation medium, end-product inhibition will be reduced.

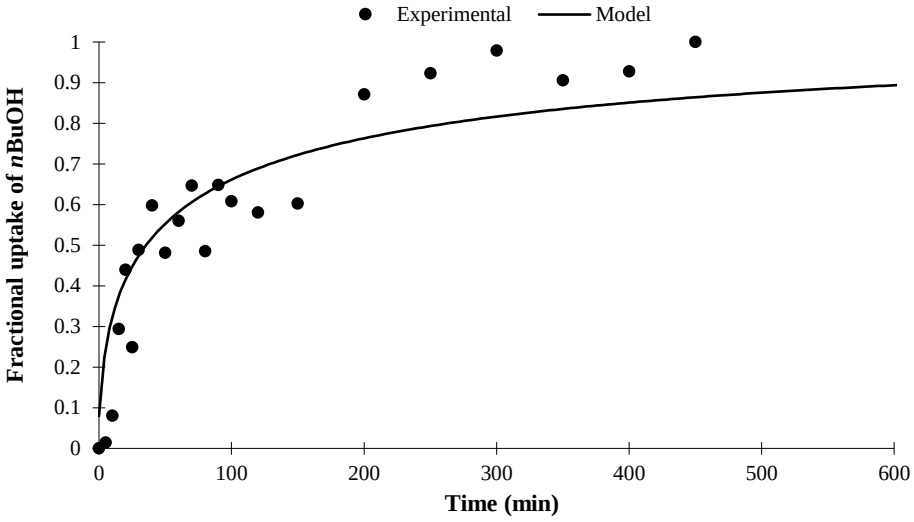

Figure 4.2: Experimental and model time course of the uptake of *n*-butanol by 5% (w/v) P(VC_{12}ImBr) in 1 L of a 2 wt% concentration *n*-butanol solution.

Internal diffusion rates for an absorbent material can be assessed through a least squares regression fit to the Crank Equation, which finds the diffusivity (D) (Crank, 1975). In this case, the pieces of P(VC_{12}ImBr) were assumed to be spherical with an average radius, known as the diffusional path length, and the Crank Equation for diffusion in a sphere was used accordingly (Crank, 1975; Pittman et al., 2015), where the diffusivity of *n*-butanol in P(VC_{12}ImBr) for this model was found to be 6.5 x 10^{-8} cm^2/s. However, as the polymer pieces are assumed to be spherical, the fit of the data to the curve is taken into consideration for accuracy.

The diffusivity of P(VC_{12}ImBr) is lower than previously found diffusivities of *n*-butanol in polymers, as listed in Table 4.3, however this is not anticipated to limit sorption due to the fast rate of uptake of 90% of the *n*-butanol within 3 hours. Compared to TPPB systems for polymers following assumptions for spherical diffusivity, P(VC_{12}ImBr) has a diffusivity that falls within the range of values for phenol in various grades of Hytrel (Pittman et al., 2015) and poly(ethylene-co-vinyl acetate) (EVA) (Amsden et al., 2002).

Table 4.3: Summary of diffusivity values relevant to this work

Polymer	Target Molecule	Diffusion Path	Diffusional Path Length (cm)	D (cm^2/s)	Source
P(VC_{12}ImBr)	*n*-Butanol	Spherical	0.54	6.5×10^{-8}	This work
Silicone rubber	*n*-Butanol	Plane sheet	0.080	6.5×10^{-7}	Watson & Payne, 1990
Polydimethylsiloxane	*n*-Butanol	Plane sheet	<0.10	3.0×10^{-7}	Cocchi et al., 2015
Hytrel 8206 L	Phenol	Spherical	0.32	1.6×10^{-7}	Pittman et al., 2015
Hytrel 5544	Phenol	Spherical	0.33	4.3×10^{-8}	Pittman et al., 2015
EVA	Phenol	Spherical	0.34	3.7×10^{-9}	Amsden et al., 2003

4.1.5 Biocompatibility

To be deemed a biocompatible material for ISPR applications, P(VC_{12}ImBr) must not inhibit the growth of the microorganisms in use, through toxicity towards the cells or removal of essential nutrients (Mirata, 2009). Both cell density and glucose consumption for *S. cerevisiae* and *C. acetobutylicum* in the presence of P(VC_{12}ImBr) were determined, as they are quantitative measurements that are commonly assessed for biocompatibility (Mao et al., 2013; Bacon et al., 2016; Collins & Daugulis, 1999). Determining the biocompatibility of P(VC_{12}ImBr) with these species were chosen as there will be implementation of ISPR in both ethanol and ABE fermentations in later work.

Figure 4.3 shows the cell densities and residual glucose levels in comparison to a positive control sample for each species. Accordingly, P(VC_{12}ImBr) does not appear to inhibit microbial growth for *S. cerevisiae* or *C. acetobutylicum* and is therefore biocompatible. These results align

with those previously reported (Bacon et al., 2017), demonstrating that this PIL is appropriate for use as an extractant in a biphasic system with these organisms.

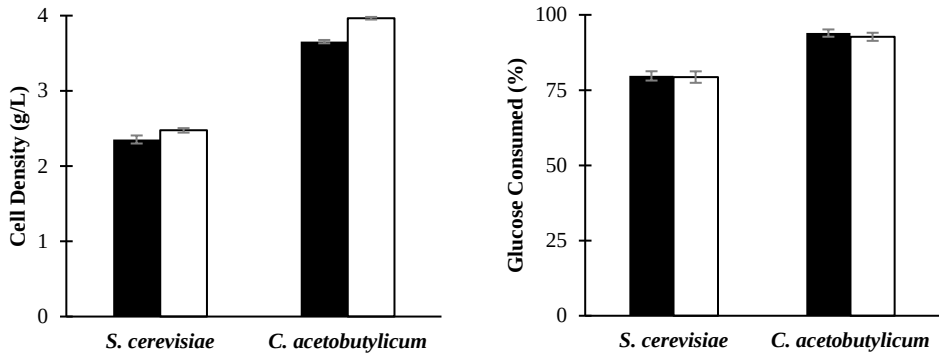

Figure 4.3: Cell density and glucose consumed after 24 hours of *S. cerevisiae* and *C. acetobutylicum* growth with (□) and without (■) the addition of 5 wt% P(VC_{12}ImBr). Error bars show standard deviation from triplicate samples (n=3).

4.1.6 Ion Exchange and Analyte Competition

As P(VC_{12}ImBr) is a polyelectrolyte, the influence of its ionic functional group was assessed, specifically the potential for ion exchange while in contact with fermentation broth that could lead to reduced sequestration of target molecules or nutrient depravation of the microorganisms in use, which has been suggested previously (Bacon et al., 2017).

To determine if P(VC_{12}ImBr) undergoes ion exchange, analysis for changes in specific ions present in aqueous ABE fermentation medium was undertaken. Table 4.4 lists the levels of these ions before and after 24-hour contact with P(VC_{12}ImBr). The difference in ion concentrations is negligible for potassium, iron, magnesium, and manganese in the medium leading to the conclusion that P(VC_{12}ImBr) does not interact with the cation species present. In contrast, Table 4.4 shows a reduction in phosphate and sulphate levels, along with the detection of bromide anions in the medium after 24 hours, suggesting that anion exchange is occurring between sulphate and phosphate with the bromide anions in P(VC_{12}ImBr) while contacting the fermentation medium. However, a molar balance calculation that accounted for the charges of these anions was performed

(Appendix C) and showed results that do not agree with the data in Table 4.4, which may be attributed to measurement error.

As biocompatibility tests have demonstrated that both *S. cerevisiae* and *C. acetobutylicum* can grow unaffected by the presence of P(VC_{12}ImBr), the reduction in phosphate and sulphate levels is not expected to reduce cell growth for this ISPR system.

Table 4.4: Summary of results for the detection of specific ions in ABE Medium B following 24 hour contact with 5% (w/v) of P(VC_{12}ImBr)

Ion	Initial Concentration (mg/L)	Final Concentration (mg/L)
K^+	260 ± 0	260 ± 0
Fe^{3+}	1.6 ± 0.3	1.7 ± 0.1
Mg^{2+}	28 ± 1	28 ± 1
Mn^+	4.3 ± 0.1	4.3 ± 0.1
SO_4^{2-}	1600 ± 0	65 ± 4
PO_4^{3-}	300 ± 0	260 ± 10
Br^-	<1.0 ± 0	740 ± 50

Note: Salts in ABE Medium B are potassium phosphate monobasic (KH_2PO_4), potassium phosphate dibasic (K_2HPO_4), magnesium sulphate heptahydrate ($MgSO_4 \bullet 7H_2O$), manganese sulphate heptahydrate ($MnSO_4 \bullet 7H_2O$), and ferrous (III) heptahydrate ($FeSO_4 \bullet 7H_2O$). Error shows standard deviation from triplicate samples (n=3).

In addition, to determine if analyte competition or ion exchange affects the PC and therefore effectiveness of P(VC_{12}ImBr) for the target fermentation products, PC testing in ABE fermentation medium was done, and it was found that *n*-butanol maintains its PC of 6.5 ± 0.4 and selectivity of 46 ± 4, along with its PCs for ethanol and acetone at 1.1 ± 0.4 and 1.3 ± 0.3, respectively (data not shown).

4.2 Biofuel fermentations with *in-situ* product removal using P(VC_{12}ImBr)

As P(VC_{12}ImBr) has been shown here to possess suitable characteristics for use as an ISPR extractant, implementation in fermentation processes would demonstrate its promising application.

Therefore, both ethanol and ABE fermentations with P(VC_{12}ImBr) were performed in attempts to reduce end-product inhibition and improve these biofuel fermentation processes, as these bioprocesses have been well-studied in the area of ISPR.

4.2.1 Batch Ethanol ISPR Fermentation with P(VC_{12}ImBr)

A control batch ethanol fermentation and one with ISPR were performed, the time courses of which can be seen in Figure 4.4. In the ISPR fermentation, circulation of the broth through a packed column containing P(VC_{12}ImBr) and back into the bioreactor at a rate of 30 mL/min was initiated at 18 hours to provide contact between the aqueous and polymer phases. Absorption of ethanol by P(VC_{12}ImBr) once ISPR began is evidenced in Figure 4.4 (b) by a drop in the aqueous ethanol concentration at the 20 hour point. Table 4.5 shows a summary comparison between the control and ISPR fermentations, in which the amount of ethanol absorbed by P(VC_{12}ImBr) in the ISPR fermentation was calculated based on its previously found PC value, along with the 5% (w/v) mass fraction of polymer that was used.

The amount of ethanol absorbed by P(VC_{12}ImBr) was determined through mass balance using the PC of P(VC_{12}ImBr) for ethanol, the mass of polymer used, and the ethanol concentration in the fermentation medium. The 5% (w/v) mass fraction of P(VC_{12}ImBr) used in the ISPR fermentation resulted in the sequestration of 17.3 g of ethanol by the polymer. The amount of absorbed ethanol was then used in calculations to determine an equivalent final product concentration based on the aqueous volume in the bioreactor.

Although P(VC_{12}ImBr) sequestered the target molecule in the ethanol ISPR fermentation, the total final ethanol concentration and subsequent volumetric productivity did not improve. The lack of improvements in the ethanol ISPR fermentation may be due to the insufficient mass fraction of P(VC_{12}ImBr) in contact with the fermentation medium, along with its modest ethanol PC value in comparison to *n*-butanol. However, to keep the level of ethanol below 50 g/L in the fermentation medium, a 50% (w/v) mass fraction of P(VC_{12}ImBr) would be required, which was determined

based on its PC. As 50 g/L ethanol is below the threshold for complete growth inhibition of *S. cerevisiae*, cell viability may be extended to increase both final ethanol concentration and volumetric productivity over the batch fermentation period of 50 hours.

Although P(VC_{12}ImBr) removed ethanol in the ISPR fermentation, its low PC requires a large amount of polymer and therefore a larger volume to potentially improve upon parameters, which may not be economically feasible. The low affinity of P(VC_{12}ImBr) for ethanol as compared to *n*-butanol, coupled with the biofuel superiority of *n*-butanol over ethanol as discussed in Section 2.2, leads to increased focus on the bioproduction of *n*-butanol through ABE fermentation.

Table 4.5: Summary of results for control and ISPR ethanol batch fermentations by *S. cerevisiae*

Parameter	Ethanol Fermentation	
	Control	**ISPR**
Fermentation time (h)	50	50
Glucose consumed (g/L)	180	160
Biomass produced (g/L)	3.3	2.6
Ethanol produced (g/L)	87	78
in aqueous phase (g)	270	240
in polymer phase (g)	-	16
Ethanol yield (g/g)	0.48	0.49
Volumetric Productivity (g/Lh)	1.8	1.6

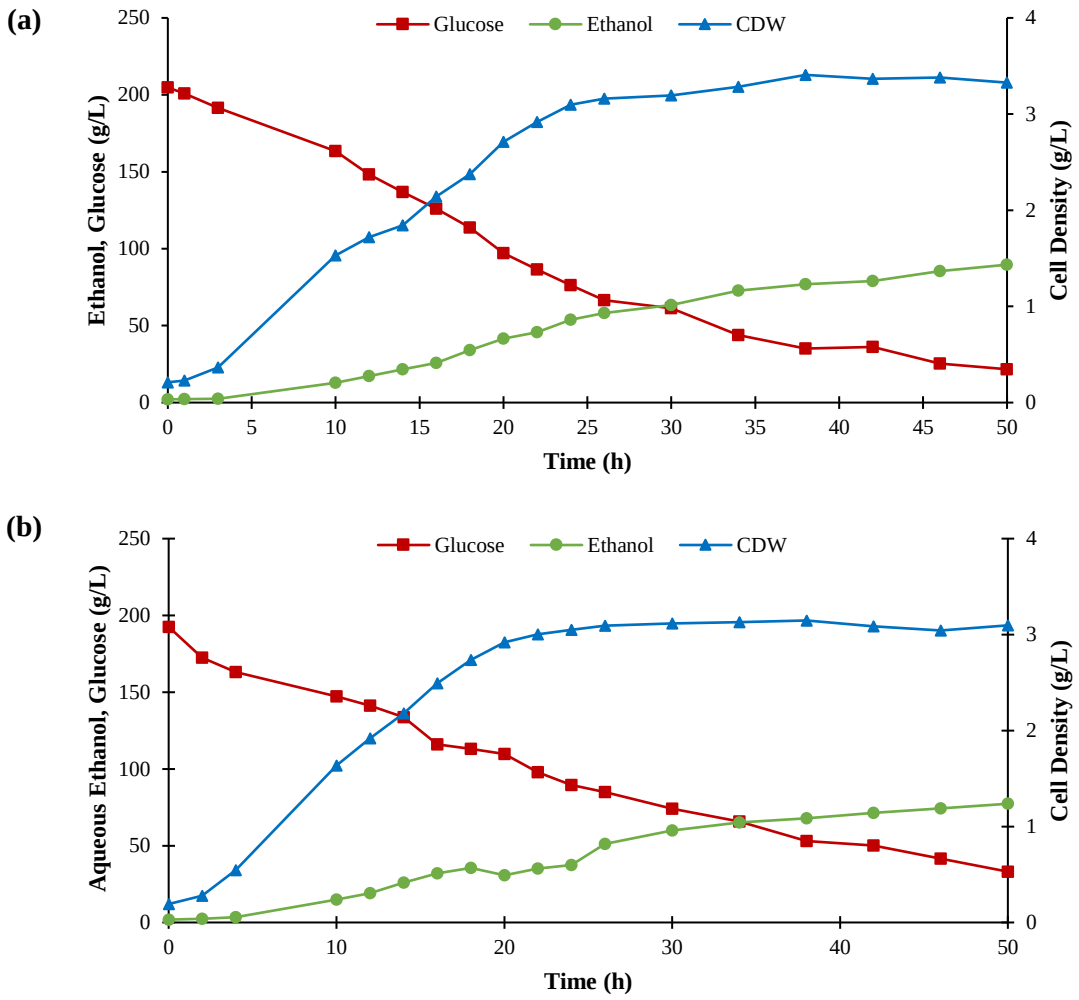

Figure 4.4: Kinetics of batch ethanol fermentations by *S. cerevisiae*; (a) control fermentation with no ISPR; (b) ISPR fermentation where contact of the fermentation broth with 5% (w/v) P(VC_{12}ImBr) was initiated at 18 hours.

4.2.2 Batch ABE ISPR Fermentation with P(VC_{12}ImBr)

To demonstrate the reduction of end-product inhibition and improvement in the ABE fermentation with P(VC_{12}ImBr), two 50-hour batch fermentations were performed, one as a control and one with ISPR, the time courses of which can be seen in Figure 4.5. The pH of the fermentation broth was not automatically controlled in order to eliminate risk of pH over-shoot (Barton & Daugulis, 1992), however the pH was monitored at each sampling time to ensure that it was between 4 and 5, as this range is optimal for solventogenesis (Huang et al., 1986). In the ISPR

fermentation, product removal occurred by initiating the flow of the aqueous broth through a packed column containing approximately 5% (w/v) P(VC_{12}ImBr) and back into the bioreactor in a closed loop at a rate of 50 mL/min. The circulation of fermentation broth was initiated amid solventogenesis at 18 hours, prior to anticipated toxic levels of *n*-butanol.

It is seen in Figure 4.5, that both the control and ISPR fermentations exhibited acidogenesis during the first 10 hours, during which acetic acid and butyric acid were mainly produced, followed by solventogenesis, with conversion of these acids to solvents, noted by the decrease in acid concentrations and increase in acetone, *n*-butanol, and ethanol concentrations. In the control fermentation, microorganism growth appeared to have slowed by 34 hours, indicative of solvent inhibition. By 38 hours into the control fermentation, approximately 5 g/L residual glucose remained until the end of the batch period. The residual glucose, along with stationary *n*-butanol, acetone, and ethanol concentrations are likely a result of end-product inhibition, ceasing production at an *n*-butanol concentration of 10 g/L. It is also important to note the dramatic decline in optical density, which may be due to cell flocculation as solvent concentrations increase in the fermentation broth (Fick & Engasser, 1986). As cell aggregation affects optical density readings, cell dry weight measurements from the calibration curve were assumed not to be accurate, and therefore this is a decline in cell optical density and not necessarily cell dry weight.

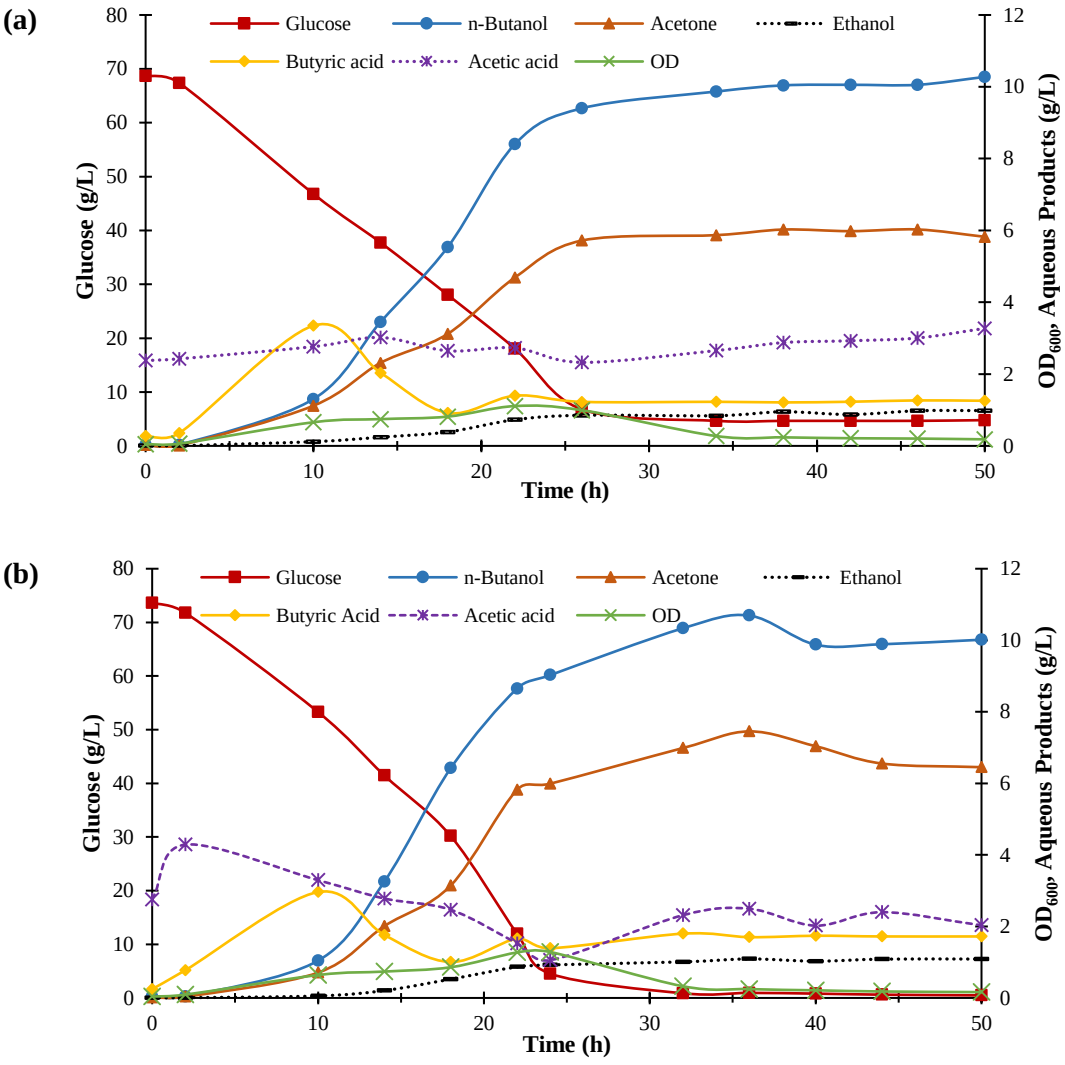

Figure 4.5: Kinetics of batch ABE fermentations by *C. acetobutylicum*; (a) control fermentation with no ISPR; (b) ISPR fermentation where contact of fermentation broth with 5% (w/v) P(VC$_{12}$ImBr) was initiated at 18 hours.

The enhancement of the ABE ISPR fermentation with P(VC$_{12}$ImBr) is evidenced in multiple ways, including the consumption of glucose, as seen in Figure 4.6. In the ISPR fermentation, glucose was consumed at a rate similar to that of the control up until the 18-hour mark, at which point P(VC$_{12}$ImBr) was introduced. At 22 hours, the glucose consumption rate reached its maximum of 4.6 g/Lh, an increase of 84% compared to the control fermentation at the same time and 61% higher than the control's maximum glucose consumption rate at 26 hours. As

there was reduced end-product inhibition, the glucose consumption rate of the ISPR fermentation peaked earlier than the control, following which it proceeded to decline until the substrate was completely consumed by 36 hours.

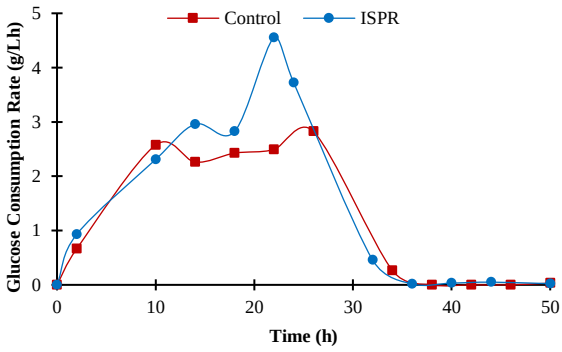

Figure 4.6: Instantaneous glucose consumption rates for control and ISPR ABE fermentations.

The absorption of *n*-butanol, acetone, and ethanol by P(VC_{12}ImBr) in the ISPR fermentation is evidenced in Figure 4.7, noted by increasing and decreasing aqueous concentrations as compared to the control fermentation. Following contact with P(VC_{12}ImBr) at 18 hours, the solvent concentration increased slightly compared to the control until 24 hours, at which point the control plateaued and the ISPR continued to increase until 36 hours, indicative of further solvent production by the cells. The following decline in the aqueous solvent concentration, along with complete consumption of glucose at 36 hours (seen in Figure 4.5) suggest that ABE production has ended and further absorption by P(VC_{12}ImBr) is occurring. Finally, a plateau of the solvent concentration level in the ISPR fermentation indicates that equilibrium has been reached between the fermentation broth and P(VC_{12}ImBr) within 3 hours, as had been demonstrated previously in Section 4.1.4. The dashed line and open symbol of the ISPR fermentation are plotted to represent the equivalent solvent concentration, beginning after the initiation of ISPR, up to the 50 hour mark, where the additional solvents absorbed by P(VC_{12}ImBr) were determined and accounted for.

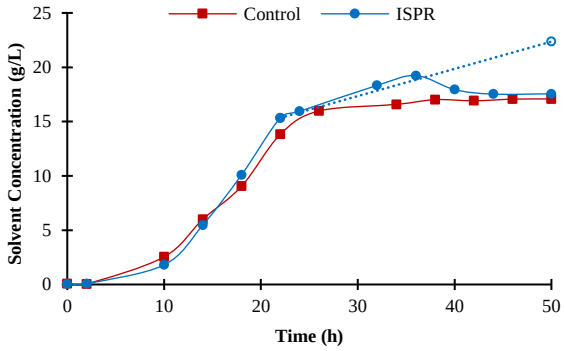

Figure 4.7: Concentration levels of total solvents (*n*-butanol, acetone, and ethanol) in the control and ISPR ABE fermentations, where the solid lines represent the aqueous solvents, and the dashed line and open symbol represent the equivalent concentration absorbed by P(VC_{12}ImBr) in the ISPR fermentation.

To determine the amount of *n*-butanol, acetone, and ethanol absorbed by P(VC_{12}ImBr) in the ISPR fermentation, mass balance calculations were performed via their respective PCs, the mass of polymer used, and their concentrations in the fermentation medium. Using approximately 5% (w/v) mass fraction (150 g) of P(VC_{12}ImBr) resulted in the absorption of 14 g *n*-butanol, 1.8 g of acetone, and 0.25 g of ethanol. The amount of solvents absorbed by P(VC_{12}ImBr) were then included in calculations to determine equivalent final product concentrations, which were based on the aqueous volume of the fermenter.

A summary and comparison of the control and ISPR ABE fermentations in this work is shown in Table 4.6. In the ISPR fermentation, a total of 14 g/L *n*-butanol, 7.0 g/L acetone, and 1.2 g/L ethanol were produced, totaling 22 g/L solvent, an increase of 22% compared to the control. Most notably, the ISPR ABE fermentation increased both *n*-butanol and total solvent volumetric productivity by 76%, as glucose was completely consumed in a reduced time period of 34 hours compared to the control fermentation. Overall, a 76% improvement in volumetric productivity of the batch ABE fermentation by *C. acetobutylicum* ATCC 824 was achieved with the addition of P(VC_{12}ImBr) through the reduction of end-product inhibition to increase production of the target molecule, *n*-butanol, as compared to the control.

Table 4.6: Summary of results for control and ISPR ABE batch fermentation by *C. acetobutylicum* ATCC 824

Parameter	ABE Fermentation	
	Control	ISPR
Fermentation time (h)	50	34
Glucose consumed (g/L)	64	73
***n*-Butanol produced (g/L)**	12	14
In aqueous phase (g)	37	46
In polymer phase (g)	-	14
Acetone produced (g/L)	5.8	7.0
In aqueous phase (g)	19	23
In polymer phase (g)	-	1.8
Ethanol Produced (g/L)	0.97	1.2
In aqueous phase (g)	3.2	3.8
In polymer phase (g)	-	0.25
Total solvent produced (g/L)	18	22
Yield (g/g)		
Total solvent	0.28	0.30
***n*-Butanol**	0.18	0.19
Volumetric productivity (g/Lh)		
Total solvent	0.37	0.65
***n*-Butanol**	0.23	0.41

In addition, through mass balance, it was determined that the aqueous solution absorbed by P(VC_{12}ImBr) in the ABE ISPR fermentation consisted of 72 wt% water, 24 wt% *n*-butanol, 3.1 wt% acetone, and 0.44 wt% ethanol, demonstrating the material's high selectivity for *n*-butanol. The selective absorption of P(VC_{12}ImBr) therefore alters the expected levels of ABE in the fermentation broth, which are typically 3:6:1, as there are higher concentrations of ethanol and acetone as compared proportionally to *n*-butanol (Figure 4.5). When taking the *n*-butanol, acetone, and ethanol absorbed by P(VC_{12}ImBr) into consideration, acetone (23 g) and *n*-butanol (46 g) are proportionate according to this ratio, however there is only half as much ethanol as expected at 3.7 g total was produced.

In comparison to other ISPR methods that have been used for ABE fermentations, the selective behaviour of P(VC_{12}ImBr) surpasses previous work in terms of product recovery from a fermentation broth, a comparison of recovered *n*-butanol can be seen in Table 4.7. The ability of P(VC_{12}ImBr) to selectively remove *n*-butanol at a phase ratio of only 5 wt% is extremely promising in terms of downstream recovery. As the recovered aqueous solution containing 24 wt% *n*-butanol is above its water solubility limit of 7.3 wt%, there is anticipated phase separation if this composition were to be removed from the polymer, resulting in a concentrated organic phase that would separate in a decanter. This *n*-butanol phase could then be purified in a single organic distillation column, which may eliminate the need for the first distillation column typically required for conventional ABE purification. This suggests that not only can the incorporation of P(VC_{12}ImBr) improve production parameters of *n*-butanol as compared to control fermentations (Table 4.6), but also improve the downstream recovery process, as has been suggested by others using ISPR (Nielsen & Prather, 2009; Xue et al., 2012).

Table 4.7: Comparison of ISPR methods in ABE fermentations for the selective removal of *n*-butanol from an initial aqueous fermentation broth to a more concentrated *n*-butanol solution in the extractant

ISPR Extractant	*n*-Butanol in Fermenter (wt%)	*n*-Butanol Content Extracted (wt%)	Source
P(VC_{12}ImBr)	1.0	24	This work
Norit ROW0.8	0.89	17	Xue et al., 2016
Dowex® Optipore SD-2	0.34	11-17	Nielsen & Prather, 2009
Gas stripping	0.8-1.3	15	Xue et al., 2012
Oleyl alcohol	0.7	3.7	Roffler et al., 1987

4.3 Recovery and Analysis of *n*-Butanol absorbed by P(VC_{12}ImBr)

The purpose of ISPR is to reduce production costs through process improvements, including downstream processing, and therefore the recovery of *n*-butanol from P(VC_{12}ImBr) was

investigated, with this focus due to the higher selectivity of the material for *n*-butanol, along with the heterogeneous azeotrope of the *n*-butanol-water system. As the purification of *n*-butanol typically involves a two-column system, as described and shown in Section 2.6, there is potential to eliminate the need for the first column if recovery of the *n*-butanol and water mixture removed from the extracting phase is above the solubility limit, and can form a separate *n*-butanol-rich organic phase. Therefore, the solubility limit of *n*-butanol in water was used as a benchmark to exceed for determining effective recovery from P(VC_{12}ImBr), first by examining the water + *n*-butanol + P(VC_{12}ImBr) ternary system over a range of initial *n*-butanol concentrations, followed by experiments to collect and measure aqueous *n*-butanol absorbed then desorbed by P(VC_{12}ImBr).

However, before examining the ternary system and the absorption and desorption characteristics of the polymer, a modified process configuration involving ISPR with P(VC_{12}ImBr) was formulated, to replace the conventional recovery system described earlier in Figure 2.1. Figure 4.8 shows the proposed layout for continuous *n*-butanol separation process using P(VC_{12}ImBr) for ISPR and only one distillation column. Following extraction of *n*-butanol by P(VC_{12}ImBr), the polymer is sent to an evaporator to thermally remove the absorbed liquid. The polymer is then recycled and sent back to be reused as an ISPR extractant, and the vapor is then condensed and sent to a decanter where phase separation occurs. From the decanter, the upper organic phase is sent to a distillation column to produce pure *n*-butanol, with water being condensed and sent back to the decanter for phase separation. The lower aqueous phase from the decanter is sent back to the polymer extraction unit to concentrate the *n*-butanol feed, with the diluted liquid going back to the bioreactor.

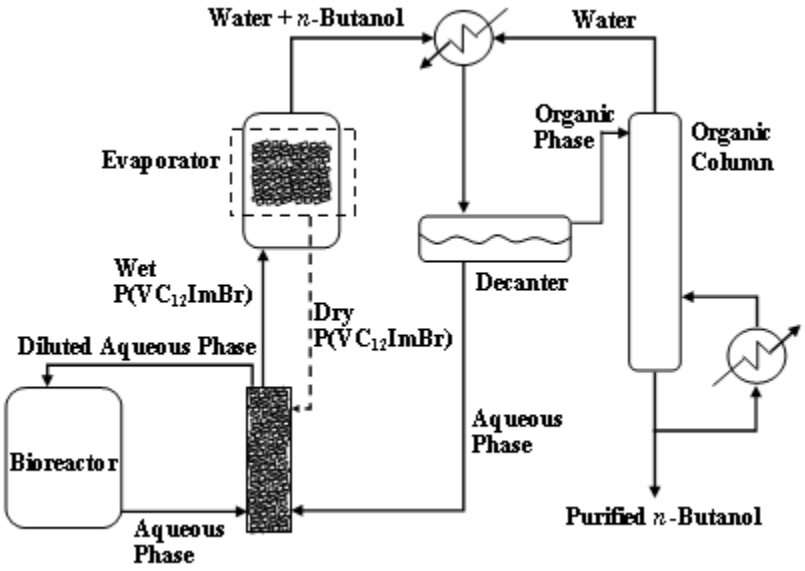

Figure 4.8: Proposed layout of continuous ABE ISPR fermentation using P(VC_{12}ImBr) with one distillation column for *n*-butanol purification.

4.3.1 Water + *n*-Butanol + P(VC_{12}ImBr) Ternary System

To determine if the *n*-butanol concentration of the liquid absorbed by P(VC_{12}ImBr) was above the solubility limit, the water + *n*-butanol + P(VC_{12}ImBr) ternary system was explored. The experimental tie lines for this ternary system at 30°C are plotted on a phase diagram in Figure 4.9, the data for which are listed in Appendix E. Each set of data represents a differing initial aqueous *n*-butanol concentration, ranging from 1 wt% to 6 wt% of the entire system, which were selected based on the potential amount of *n*-butanol accumulated in an ABE fermentation, along with being below the solubility limit of *n*-butanol in water. For each system, there are two distinct phases at equilibrium as *n*-butanol and water partitioned into P(VC_{12}ImBr), one phase consisting of just water and *n*-butanol, and one phase consisting of water, *n*-butanol, and P(VC_{12}ImBr).

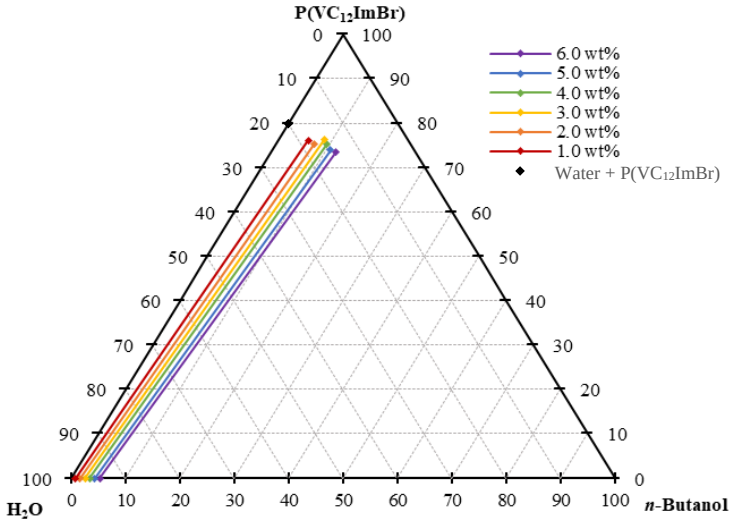

Figure 4.9: Ternary diagram (in wt%) constructed by experimental data of the water + *n*-butanol + P(VC_{12}ImBr) system at equilibrium with a consistent polymer mass fraction at 5% (w/v) and varying initial *n*-butanol concentration.

The selectivity of P(VC_{12}ImBr) considers the water and *n*-butanol content in the polymer phase, which was found through mass balance calculations from the ternary phase data and is displayed in Figure 4.10. As the system's aqueous content of *n*-butanol increased from 1.0 wt% to 6.0 wt%, the *n*-butanol concentration absorbed by P(VC_{12}ImBr) increased linearly from 23 wt% to 45 wt%. These data suggest that P(VC_{12}ImBr) will preferentially take up *n*-butanol relative to water as *n*-butanol content in the system increases, which is beneficial in an ABE fermentation if using a genetically engineered organism that can tolerate higher *n*-butanol concentrations, therefore producing and recovering higher concentrations of *n*-butanol. In addition, the data in Figure 4.10 show that for each system tested, P(VC_{12}ImBr) absorbed concentrations of *n*-butanol well above the solubility limit of 7.3 wt% *n*-butanol. These high concentrations would separate into a water-rich phase and *n*-butanol-rich phase if the mixture were to be desorbed, and could therefore by fed directly to a decanter, as in the proposed process flow diagram shown in Figure 4.8.

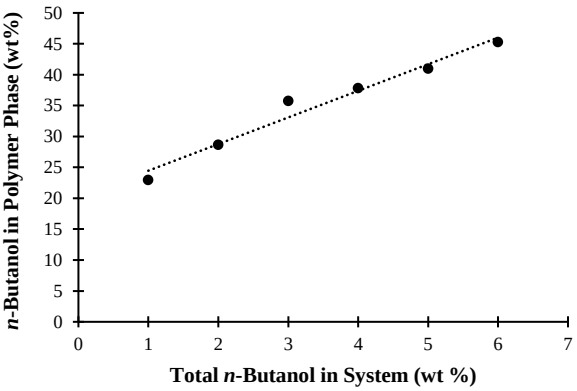

Figure 4.10: Content of *n*-butanol absorbed by P(VC_{12}ImBr) at equilibrium in relation to the total *n*-butanol content of the system.

4.3.2 Recovery of *n*-Butanol from P(VC_{12}ImBr)

The recovery of *n*-butanol from P(VC_{12}ImBr) through thermal desorption was investigated to determine whether an absorbed solution can be above the solubility limit of *n*-butanol in water when it is condensed. In a system beginning with 1.5 wt% *n*-butanol, thermal desorption of *n*-butanol and water from P(VC_{12}ImBr) yielded a product that separated into two distinct phases of different colours, as seen in Figure 4.11. The separation into phases suggests that this recovered composition was likely above the *n*-butanol + water solubility limit, as expected from Figure 4.10, in which the aqueous phase is 7.3 wt% *n*-butanol and the organic phase is 79.7 wt% *n*-butanol. However, as *n*-butanol is colourless in its pristine state, the pale yellow colour of the organic phase is possibly caused by the degradation of P(VC_{12}ImBr) during thermal exposure in the microwave or contamination from the tubing used in the experimental setup.

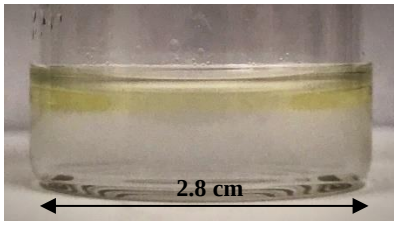

Figure 4.11: Recovered liquid from equilibrated P(VC_{12}ImBr) through experimental procedure.

The *n*-butanol-water mixture that was thermally removed from P(VC_{12}ImBr) as seen in Figure 4.11 consisted of 25.0 wt% *n*-butanol overall, which separated into two phases at equilibrium. This composition is lower than the anticipated concentration recovered from P(VC_{12}ImBr) of 28.8 wt%, which was determined through mass balance calculations using the known initial system composition, with losses attributed to potential product loss within the experimental set-up. As well, it was determined through calculations that the organic phase volume ratio of the recovered sample shown in Figure 4.11 was 32.7 vol%, with the mass balance found in Appendix E.

As this recovered *n*-butanol-water mixture from an expected ISPR scenario is above the solubility limit of *n*-butanol in water, it could be vaporized from the P(VC_{12}ImBr), condensed, and fed directly to the decanter as suggested in Figure 4.8, the proposed improved distillation system. The use of P(VC_{12}ImBr) would then eliminate the need for the first distillation column that is used to bring a dilute *n*-butanol-water solution to its azeotropic composition (Luyben, 2008). The system described by Luyben (2008) is the 'best case' in a two-column distillation system, as the azeotrope is the highest concentration achievable through distillation when beginning with a solution that is below the solubility limit of *n*-butanol in water, such as in an ABE fermentation.

The amount of *n*-butanol absorbed by and recovered from P(VC_{12}ImBr) can be compared to the condensed stream leaving the first distillation column in the two-column *n*-butanol distillation system described by Luyben (2008), as seen in Table 4.8. This two-column distillation process begins with a dilute aqueous feed that is distilled to a vapour at its azeotropic composition of around 59.9 wt% *n*-butanol, which is then condensed and sent to the decanter (Luyben, 2008). The azeotropic composition of the *n*-butanol-water system is above what was achieved in the recovery from P(VC_{12}ImBr) of 25.0 wt% *n*-butanol in this work. Furthermore, the organic phase volume fraction in the decanter achieved from the azeotropic composition is higher at 75.5 vol% compared to 32.7 vol% in this work. In both this work and by Luyben (2008), the compositions of

the organic phases are at the solubility limit (79.9 wt% *n*-butanol), and therefore an increased organic phase volume fraction in the decanter is due to an increased composition of the original vapor stream leaving P(VC_{12}ImBr) or the first distillation column.

Furthermore, Table 4.8 compares the fraction of the original *n*-butanol content that is sent to the organic distillation column in this work to Luyben (2008). The amount of *n*-butanol that is sent for distillation is related to the original composition of the vaporized stream that is condensed and then sent to the decanter, which then governs the organic phase volume fraction. As the compositions of the organic phases are at the solubility limit, the fractions of *n*-butanol sent to the organic distillation column are due entirely to the phase volume fractions. In this work, 82.3% of the *n*-butanol recovered from P(VC_{12}ImBr) would be captured in the organic phase and sent to the distillation column, whereas a higher amount of 96.7% of the *n*-butanol is sent to the second column in the two-column system from having an increased organic phase volume fraction. However, due to the selectivity of P(VC_{12}ImBr), increased initial concentrations of *n*-butanol increase the content of *n*-butanol absorbed by this polymer (Figure 4.10), and sequestering *n*-butanol from increased concentrations that are still below the *n*-butanol-water solubility limit can bring the organic phase volume fraction closer to that achieved by the composition on the *n*-butanol-water azeotrope. Therefore, the absorption of a larger organic phase volume fraction would demonstrate improvements to the *n*-butanol purification process.

Table 4.8: Comparison of *n*-butanol recovered for proposed distillation systems

	Luyben (2008)	**This Work**
Composition of Vaporized Stream		
***n*-Butanol (wt%)**	59.9	25.0
Water (wt%)	40.1	75.0
Organic Phase Fraction of Condensate (vol%)	75.5	32.7
Fraction of *n*-Butanol Sent to Organic Distillation Column (%)	96.7	82.3

Note: Sample calculations for this work are in Appendix E

4.4 References

Amsden, B.G., Bochanysz, J., & Daugulis, A.J. (2003). Degradation of xenobiotics in a partitioning bioreactor in which the partitioning phase is a polymer. *Biotechnology and Bioengineering, 84*(4), 399-405.

Bacon, S.L., Parent, J.S., & Daugulis, A.J. (2014). A framework to predict and experimentally evaluate polymer-solute thermodynamic affinity for two-phase partitioning bioreactor (TPPB) applications. *Journal of Chemical Technology and Biotechnology, 89*(7), 948-956.

Bacon, S.L., Daugulis, A.J., & Parent, J.S. (2016). Isobutylene-rich imidazolium ionomers for use in two-phase partitioning bioreactors. *Green Chemistry, 18*(24), 6586-6595.

Bacon, S.L., Ross, R.J., Daugulis, A.J., & Parent, J.S. (2017). Imidazolium-based polyionic liquid absorbents for bioproduct recovery. *Green Chemistry, 19*(21), 5203-5213.

Barton, W. E., & Daugulis, A. (1992). Evaluation of solvents for extractive butanol fermentation with *Clostridium acetobutylicum* and the use of poly(propylene glycol) 1200. *Applied Microbiology and Biotechnology*, *36*(5), 632–639.

Bruce, L.J., & Daugulis, A.J. (1991). Solvent selection strategies for extractive biocatalysis. *Biotechnology Progress, 7*(2), 116-124.

Cocchi, G., De Angelis, M.G., & Doghieri, F. (2015). Solubility and diffusivity of liquids for food and pharmaceutical applications in crosslinked polydimethylsiloxane (PDMS) films: I. Experimental data on pure organic components and vegetable oil. *Journal of Membrane Science, 492,* 600-611.

Collins, L.J., & Daugulis, A.J. (1999). Benzene/toluene/p-xylene degradation. Part I. Solvent selection and toluene degradation in a two-phase partitioning bioreactor. *Applied Microbiology and Biotechnology, 52*(3), 354-359.

Crank, J. (1975). *The mathematics of diffusion*. New York: Academic Press.

Fick, M., & Engasser, J-M. (1986). The deflocculating effect of chloride salts (ions) on *Clostridium acetobutylicum* grown in continuous cultures. *Applied Microbiology and Biotechnology, 25*(3): 194-196.

González-Peñas, H., Lu-Chau, T.A., Moreira, M.T., & Lema, J.M. (2014). Solvent screening methodology for in situ ABE extractive fermentation. *Applied Microbiology and Biotechnology, 98*(13), 5915-5924.

Huang, L., Forsberg, C.W., & Gibbins, L.N. (1986). Influence of external pH and fermentation products on *Clostridium acetobutylicum* intracellular pH and cellular distribution of fermentation products. *Applied and Environmental Microbiology, 51*(6), 1230-1234.

Jiménez-Bonilla, P., & Wang, Y. (2018). *In situ* biobutanol recovery from clostridial fermentations: a critical review. *Critical Reviews in Biotechnology, 38*(3), 469-482.

Jones, D. T., & Woods, D. R. (1986). Acetone-butanol fermentation revisited. *Microbiological Reviews*, *50*(4), 484–524.

Littlejohns, J.V., & Daugulis, A.J. (2008). Response of a solid-liquid two-phase partitioning bioreactor to transient BTEX loadings. *Chemosphere*, *73*(9), 1453-1460.

Lufrano, F., Gatto, I., Staiti, P., Antonucci, V., & Passalacqua, E. (2000). Sulfonated polysulfone ionomer membranes for fuel cells. *Solid State Ionics, 145*(1-4), 47-51.

Luyben, W.L. (2008). Control of the heterogeneous azeotropic *n*-butanol/water distillation system. *Energy & Fuels, 22*(6), 4249-4258.

Malinowski, J.J., & Daugulis, A.J. (1994). Salt effects in extraction of ethanol, 1-butanol and acetone from aqueous solutions, *AIChE Journal, 40*(9), 1459-1465.

Mao, S., Hua, B., Wang, N., Hu, X., Ge, Z., Li, Y., … Lu, F. (2013). 11α hydroxylation of 16α, 17-epoxyprogesterone in biphasic ionic liquid/water system by Aspergillus ochraceus. *Journal of Chemical Technology and Biotechnology*, *88*(2), 287–292.

Matsumura, M., Kataoka, H., Sueki, M, & Araki, K. (1988). Energy saving effect of pervaporation using oleyl alcohol liquid membrane in butanol purification. *Bioprocess Engineering, 3*(2), 93-100.

Mirata, M.A., Heerd, D., & Schrader, J. (2009). Integrated bioprocess for the oxidation of limonene to perillic acid with *Pseudomonas putida* DSM 12264. *Process Biochemistry*, *44*(7), 764-771.

Nielsen, D. R., & Prather, K. J. (2009). *In situ* product recovery of *n*-butanol using polymeric resins. *Biotechnology and Bioengineering*, *102*(3), 811–821.

Parent, J.S., Capela, M, Dafoe, J.T., & Daugulis, A.J. (2012). First principles approach to identifying polymers for use in two-phase partitioning bioreactors. *Journal of Chemical Technology and Biotechnology, 87*(8), 1059-1065

Pittman, M. J., Bodley, M. W., & Daugulis, A. J. (2015). Mass transfer considerations in solid-liquid two-phase partitioning bioreactors: a polymer selection guide. *Journal of Chemical Technology & Biotechnology*, *90*(8), 1391–1399.

Watson, J.M., & Payne, P.A. (1990). A study of organic compound pervaporation through silicone rubber. *Journal of Membrane Science, 49*(2), 171-205.

Xue, C., Liu, F., Xu, M., Tang, I., Zhao, J., Bai, F. & Yang, S. (2016). Butanol production in acetone-butanol-ethanol fermentation with *in situ* product recovery by adsorption. *Bioresource Technology*, *219*, 158-168.

Xue, C., Zhao, J., Lu, C., Yang, S. T., Bai, F., & Tang, I. C. (2012). High-titer *n*-butanol production by *Clostridium acetobutylicum* JB200 in fed-batch fermentation with intermittent gas stripping. *Biotechnology and Bioengineering*, *109*(11), 2746–2756.

Yerushalmi, L., & Volesky, B. (1987). Culture conditions for growth and solvent biosynthesis by a modified *Clostridium acetobutylicum*. *Applied Microbiology and Biotechnology, 25*(6), 513-520.

Chapter 5

Conclusions and Recommendations for Future Work

5.1 Conclusions

The aim of this work was to improve the processes involved in the bioproduction of ethanol by *Saccharomyces cerevisiae* and *n*-butanol by *Clostridium acetobutylicum* as biofuels via *in-situ* product removal (ISPR) with poly(vinyldodecylimidazolium bromide) [P(VC_{12}ImBr)]. P(VC_{12}ImBr), a polyionic liquid, was chosen as a two-phase partitioning bioreactor (TPPB) extractant based on promising results in previous work by Bacon et al. (2017) for sequestration of the target molecules in question, particularly *n*-butanol.

First, P(VC_{12}ImBr) was synthesized and formed into small, bead-like pieces with dimensions of approximately 2 mm by 9 mm by 6 mm, for characterization and ISPR experiments. P(VC_{12}ImBr) was found to have a partition coefficient (PC) and selectivity (α) of 1.1 and 7.2 for ethanol and 6.5 and 46 for *n*-butanol, respectively, demonstrating that this material has a stronger affinity for *n*-butanol, which led to a focus on improving its production. As a semi-crystalline polymer, a differential scanning calorimetry (DSC) scan of P(VC_{12}ImBr) found its T_m of -17°C and a T_g above 200°C, which is very high compared to other absorptive polymers, and therefore, can be plasticized in water to reduce its T_g. The diffusivity of *n*-butanol in P(VC_{12}ImBr) was found to be in the same range of other absorptive materials at 6.51 x 10^{-8} cm^2/s, absorbing 90% *n*-butanol within 3 hours to reduce inhibitory levels, which is appropriate for the biological rate of *C. acetobutylicum* in an ABE fermentation. In addition, P(VC_{12}ImBr) was found to be biocompatible with both *S. cerevisiae* and *C. acetobutylicum,* which was determined by optical density and glucose consumption measurements. During experiments involving the possibility of ion exchange between medium components and P(VC_{12}ImBr), a reduction in sulphate and phosphate and an increase in bromide levels in medium suggested that anion exchange between P(VC_{12}ImBr) and

the fermentation medium was occurring, however it did not seriously affect its use in subsequent experiments, as the polymer still maintained its PC and selectivity for *n*-butanol, ethanol, and acetone.

Following the characterization of P(VC_{12}ImBr), this material was utilized as the absorptive material in ethanol and ABE fermentations. Relative to a control batch ethanol fermentation, *in-situ* product removal using P(VC_{12}ImBr) indicated absorption of ethanol once contact began, however no improvement in the volumetric productivity was observed, which is attributed to the small mass fraction of P(VC_{12}ImBr) used. A calculation showed that using a 50% (w/v) rather than a 5% (w/v) phase volume fraction of P(VC_{12}ImBr) would likely reduce inhibitory levels of ethanol and lead to improved fermentation kinetics. Relative to a control batch acetone-butanol-ethanol (ABE) fermentation, the use of P(VC_{12}ImBr) in ISPR sequestered *n*-butanol to reduce end-product inhibition and showed improved performance. The ABE ISPR fermentation resulted in an increased final product concentration of 22% and increased volumetric productivity of 76% as compared to the control ABE fermentation. The use of P(VC_{12}ImBr) also sequestered *n*-butanol to a concentrated solution for recovery greater than previous studies employing ISPR in an ABE fermentation, as a solution consisting of 24 wt% *n*-butanol was extracted by P(VC_{12}ImBr) from the fermentation broth.

Finally, P(VC_{12}ImBr) demonstrated potential improvement to the recovery and purification of *n*-butanol through its selective behaviour. First, the water + *n*-butanol + P(VC_{12}ImBr) ternary system phase diagram was constructed, with the aim of determining if the liquid absorbed by P(VC_{12}ImBr) is above the solubility limit. The phase diagram showed the material preferentially absorb *n*-butanol over water as the overall content of *n*-butanol in the system increased, which is important for reducing inhibitory levels in an ABE fermentation, suggesting that the use of organisms with a higher tolerance for *n*-butanol could be highly beneficial for downstream recovery purposes. Furthermore, P(VC_{12}ImBr) absorbed *n*-butanol at concentrations above its solubility

limit, which resulted in phase separation between *n*-butanol and water once the solution was thermally removed and condensed. This concentrated *n*-butanol solution recovered from P(VC_{12}ImBr) has the potential to eliminate one distillation column as compared to the standard two-column distillation system for dilute ABE fermentation broth purification.

5.2 Recommendations for Future Work

The investigation of P(VC_{12}ImBr) as an ISPR extractant for ethanol and *n*-butanol biofuel fermentation processes has delivered promising results thus far, however the use of this material is still inchoate, and its synthesis and characterization can be expanded. For example, for P(VC_{12}ImBr) to maintain its affinity and selectivity, polymer synthesis and forming into pieces for application should be further examined for quality control purposes, as the current method does not produce identical bead-like pieces, as slight variation is seen in Figure 3.1.

As well, investigation into the reusability of P(VC_{12}ImBr) following multiple instances of anion exchange with fermentation broth, along with repeated thermal product recovery is necessary, for determining how many cycles of reuse the material can withstand. The reusability of P(VC_{12}ImBr) in the production of biofuels is particularly important as both *n*-butanol and ethanol are low value products (Kamm & Kamm, 2004). Therefore, in order for biofuel production utilizing P(VC_{12}ImBr) in ISPR to be economically viable processes, reuse of this material is necessary.

Integrating the ISPR ABE fermentation and the *n*-butanol separation process in a continuous process, as described in Section 4.3, is a major step towards improving the overall production of *n*-butanol with P(VC_{12}ImBr). Continuously recycling P(VC_{12}ImBr) after thermal separation to remove *n*-butanol from the fermentation broth may allow for improved volumetric productivity, energy efficiency, and ultimately reduced production costs. Furthermore, the integrated ABE fermentation and recovery process can be enhanced in other areas of the fermentation to improve upon its parameters. These areas include microbial strain modification and

engineering, where *n*-butanol-producing microorganisms have been mutated to have an increased tolerance to *n*-butanol, using alternative substrates including agricultural byproducts and waste to reduce costs, or modifying the cell configuration via immobilization or cell recycle to increase cell concentration in a bioreactor (Ezeji et al., 2007).

5.3 References

Bacon, S.L., Ross, R.J., Daugulis, A.J., & Parent, J.S. (2017). Imidazolium-based polyionic liquid absorbents for bioproduct recovery. *Green Chemistry, 19*(21), 5203-5213.

Ezeji, T.C., Qureshi, N., & Blaschek, H.P. (2007). Bioproduction of butanol from biomass: from genes to bioreactors. *Current Opinion in Biotechnology, 18*(3), 220-227.

Kamm, B., & Kamm, M. (2004). Principles of biorefineries. *Applied Microbiology and Biotechnology, 64*(2), 137–145.

Yang, X., Tsai, G., & Tsao, G.T. (1994). Enhancement of in situ adsorption on the acetone-butanol fermentation by *Clostridium acetobutylicum. Separations Technology, 4*(2), 81-92.

Appendix A

Cell Dry Weight Calibration Curves

Cell dry weight calibration curves were used to determine the microorganism concentration in a fermentation broth. For each sample, the cell dry weight was correlated with an optical density value.

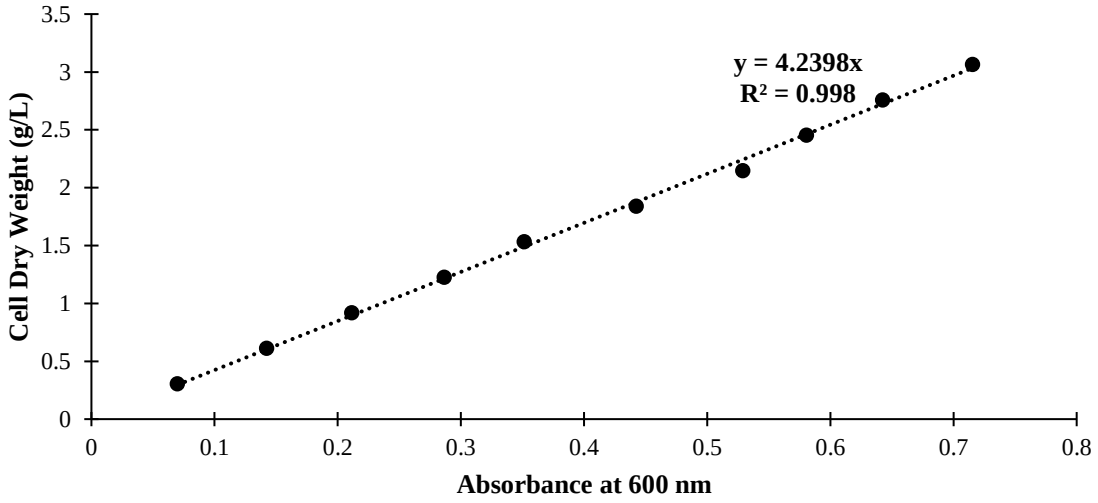

Figure A.1: Calibration curve for determination of *Saccharomyces cerevisiae* cell dry weight using optical density measurements at 600 nm with a spectrophotometer.

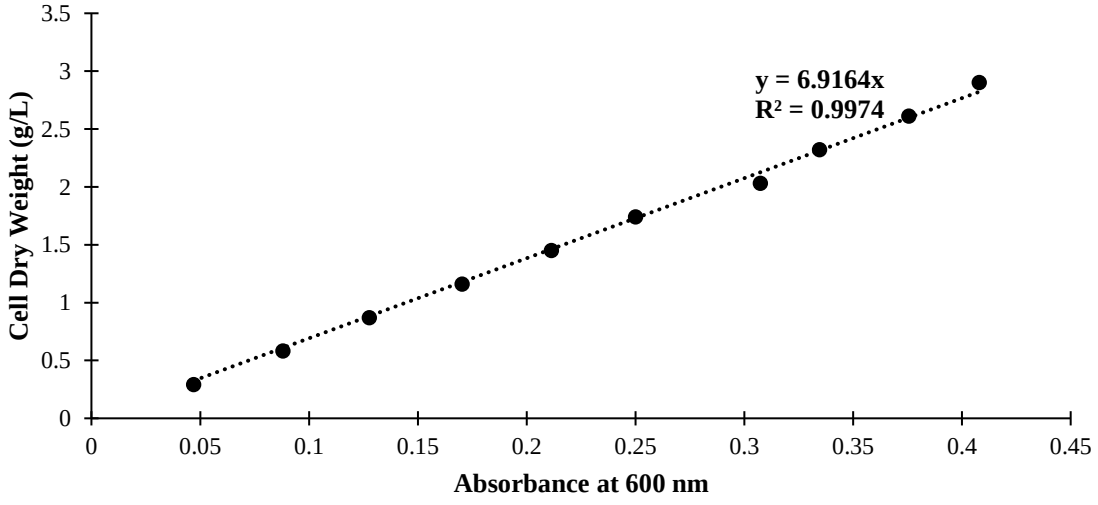

Figure A.2: Calibration curve for determination of *Clostridium acetobutylicum* cell dry weight using optical density measurements at 600 nm with a spectrophotometer.

Appendix B

Partition Coefficient and Selectivity Calculations

The following is an example calculation for the determination of the partition coefficient (PC) and selectivity (α) of P(VC_{12}ImBr) for *n*-butanol. The known values used for the calculations are listed below.

Variable	Description	Value
m_w^p	Mass of water-soaked P(VC_{12}ImBr)	0.514 g
m_{eq}^p	Mass of P(VC_{12}ImBr) at equilibrium	0.536 g
m_d^p	Mass of dry P(VC_{12}ImBr)	0.405 g
m_{eq}^{aq}	Mass of aqueous phase at equilibrium	9.79 g
V_i^{aq}	Initial volume of liquid in aqueous phase	0.0100 L
V_t^{aq}	Total volume of liquid (including water in polymer)	0.0101 L
V_{eq}^{aq}	Equilibrium volume of aqueous phase	0.00979 L
C_l	Initial concentration of *n*-butanol	10.4 g/L
C_{eq}	Equilibrium concentration of *n*-butanol	7.55 g/L

First, the initial mass of *n*-butanol in the aqueous phase was found from the initial aqueous volume and concentration:

$$m_{nBuOH}^t = (V_{aq}^i)(C_l) = (0.0100\ L)\left(10.4\frac{g}{L}\right) = 0.104\ g$$

Next the mass of *n*-butanol in the aqueous phase at equilibrium was determined from the equilibrium aqueous volume and concentration:

$$m_{nBuOH}^{aq} = \left(V_{aq}^{eq}\right)\left(C_{eq}\right) = (0.00979\ L)\left(7.55\frac{g}{L}\right) = 0.0739\ g$$

Then, the weight fraction of *n*-butanol in the aqueous phase at equilibrium was determined from the mass of *n*-butanol at equilibrium:

$$w_{nBuOH}^{aq} = \frac{m_{nBuOH}^{aq}}{m_{eq}^{aq}} = \frac{0.0739\ g}{9.79\ g} = 0.00755\ g/g$$

Then, the mass of *n*-butanol absorbed by P(VC_{12}ImBr) at equilibrium was determined through a mass balance calculation:

$$m_{nBuOH}^{p} = m_{nBuOH}^{t} - m_{nBuOH}^{aq} = 0.104\ g - 0.0753\ g = 0.0285\ g$$

Then, the weight fraction of *n*-butanol in P(VC_{12}ImBr) at equilibrium was found using the mass of *n*-butanol in the polymer and total mass of polymer at equilibrium:

$$w_{nBuOH}^{p} = \frac{m_{nBuOH}^{p}}{m_{eq}^{p}} = \frac{0.0285\ g}{0.536\ g} = 0.0532$$

The PC of P(VC_{12}ImBr) for *n*-butanol was then determined using the equilibrium weight fractions of *n*-butanol in the polymer phase and in the aqueous phase:

$$PC_{nBuOH} = \frac{w_{nBuOH}^{p}}{w_{nBuOH}^{aq}} = \frac{0.0532\ g/g}{0.00755\ g/g} = 7.04$$

To calculate the selectivity of P(VC_{12}ImBr) for *n*-butanol, the PC of P(VC_{12}ImBr) for water needed to be determined. First, the mass of water absorbed by P(VC_{12}ImBr) was found through a mass balance:

$$m_{water}^{p} = m_{eq}^{p} - m_{d}^{p} - m_{nBuOH}^{p} = 0.536\ g - 0.405\ g - 0.0285\ g = 0.103\ g$$

Then, the weight fraction of water absorbed by P(VC_{12}ImBr) at equilibrium was determined using the mass of water in the polymer and the total mass of polymer at equilibrium:

$$w_{water}^{p} = \frac{m_{water}^{p}}{m_{eq}^{p}} = \frac{0.103\ g}{0.536\ g} = 0.192\ g/g$$

Next, the weight fraction of water in the aqueous phase at equilibrium was found through a mass balance:

$$w_{water}^{aq} = 1 - w_{nBuOH}^{aq} = 1 - 0.00755\frac{g}{g} = 0.99245$$

The PC of P(VC_{12}ImBr) for water was then determined using the weight fractions of water in the polymer and aqueous phases:

$$PC_{water} = \frac{w_{water}^{p}}{w_{water}^{aq}} = \frac{0.192\ g/g}{0.99245\ g/g} = 0.193$$

Finally, the selectivity of P(VC_{12}ImBr) for *n*-butanol was calculated using the PCs of P(VC_{12}ImBr) for *n*-butanol and water:

$$\alpha_{nBuOH} = \frac{PC_{nBuOH}}{PC_{water}} = \frac{7.04}{0.193} = 36.5$$

Appendix C

Ion Exchange Calculations

The following shows the methodology for performing molar balance calculations for sulphate, phosphate, and bromide anions in the ion exchange experiments from Section 4.1.6. From Table 4.4, the initial and final aqueous concentrations of the anions present are converted to molar quantities and assuming 1 L volume.

Ion	Initial mols	Final mols	Δ mols	Total
SO_4^{2-}	0.0167	0.000677	-0.0160	0.0164 out
PO_4^{3-}	0.00316	0.00273	-0.000421	
Br^-	0	0.00926	+0.00926	0.00926 in

As the charges of sulphate (-2) and phosphate (-3) are not the same as the charge of bromide (-1), the change in mols of these anions leaving and entering the aqueous medium should not be equal, where $0.0164 \neq 0.00926$. Therefore, the charges of these anions are accounted for to be:

Ion	Δ mols	Charge	Total
SO_4^{2-}	-0.0160	-0.0320	0.332 out
PO_4^{3-}	-0.000421	-0.00126	
Br^-	+0.00926	0.00926	0.00926 in

When accounting for the charges of the free anions, $0.332 \text{ out} \neq 0.00926 \text{ in}$, which does not follow the expected results. In addition, as there is no change in aqueous cation concentrations listed in Table 4.4, these results do not agree, which may be attributed by error in ion detection.

Appendix D

Fermentation Calculations

The following calculations show the methodology of determining the total concentration produced in a batch fermentation of a target molecule, while including the content absorbed by P(VC_{12}ImBr). These values are then further used in determining the kinetics of the ISPR fermentation, including the yield, volumetric productivity, and glucose consumption rate. The following example is *n*-butanol uptake by P(VC_{12}ImBr) in the batch ABE ISPR fermentation from Section 4.2.2.

D1.1 Uptake of Target Molecules by P(VC_{12}ImBr)

The partition coefficient (PC) was found in Section 4.1.1 by:

$$PC_{nBuOH} = \frac{w_{nBuOH}^{p}}{w_{nBuOH}^{aq}}$$

where w_{nBuOH}^{aq} and w_{nBuOH}^{p} are the weight fractions of *n*-butanol in the aqueous phase and polymer phase, respectively. The PC of P(VC_{12}ImBr) for *n*-butanol was determined to be 6.5, and thus was used for further calculations. The PC, along with other known values for calculations are listed below.

Variable	Description	Value
PC_{nBuOH}	PC of P(VC_{12}ImBr) for *n*-butanol	6.5
m_t^p	Mass of P(VC_{12}ImBr) at equilibrium	207.7 g
m_l^{aq}	Mass of liquid phase at equilibrium	3193.5 g
V_f	Total volume of liquid	3.2 L
C_l	Concentration of *n*-butanol in liquid phase	10.0 g/L

First, the mass of *n*-butanol in the aqueous phase at equilibrium was determined:

$$m_{nBuOH}^{aq} = (C_l)(V_f) = \left(10.0\frac{g}{L}\right)(3.2\ L) = 32.2\ g$$

Next, the weight fraction of *n*-butanol in the aqueous phase was determined:

$$w_{nBuOH}^{aq} = \frac{m_{nBuOH}^{aq}}{m_l^{aq}} = \frac{32.1\ g}{3193.5\ g} = 0.010\ g/g$$

Then, the weight fraction of *n*-butanol in the polymer phase was found:

$$w_{nBuOH}^{p} = (PC)\left(w_{nBuOH}^{aq}\right) = (6.5)(0.010\ g/g) = 0.065\ g/g$$

Then, the mass of *n*-butanol in the polymer was determined:

$$m_{nBuOH}^{p} = (w_{nBuOH}^{poly})\left(m_t^p\right) = \left(0.065\ \frac{g}{g}\right)(207.7\ g) = 13.6\ g$$

Following the determination of n-butanol in the polymer phase, the total mass of polymer was determined:

$$m_{nBuOH}^{t} = \ m_{nBuOH}^{p} + m_{nBuOH}^{aq} = 32.1\ g + 13.6\ g = 45.7\ g$$

Finally, the total concentration of *n*-butanol produced in the ISPR ABE fermentation was determined:

$$C_t = \frac{m_{nBuOH}^{t}}{V_f} = \frac{45.7\ g}{3.3\ L} = 13.8\ g/L$$

D1.2 Fermentation Kinetics

The following calculations show the determination of the parameters of the ABE ISPR fermentation, specifically for *n*-butanol. Known values are listed in the table below.

Variable	Description	Value
ΔS	Glucose consumed	241.4 g
ΔP	*n*-Butanol produced	45.7 g
t	Fermentation time	38 h
V_f	Total volume of liquid	3.2 L

To determine the yield of *n*-butanol by glucose consumed:

$$Y_{\frac{P}{S}} = \frac{\Delta P}{\Delta S} = \frac{45.7\ g}{241.4\ g} = 0.19\frac{g}{g}$$

To determine the volumetric productivity of *n*-butanol:

$$Volumetric\ Productivity = \frac{\Delta P}{(V_f)(t)} = \frac{45.7\ g}{(3.2\ L)(38\ h)} = 0.37\ g/Lh$$

In addition, the instantaneous glucose consumption rate for the ABE ISPR fermentation at 22 hours was determined using the known variables below:

Variable	Description	Value
$S_{t=22}$	Glucose consumed at 22 hours	61.7 g/L
$S_{t=18}$	Glucose consumed at 18 hours	43.5 g/L

$$Instantaneous\ Glucose\ Consumption\ Rate = \frac{S_{t=22} - S_{t=18}}{t_{22} - t_{18}} = \frac{61.7\frac{g}{L} - 43.5\frac{g}{L}}{22\ h - 18\ h} = 4.6\frac{g}{Lh}$$

Appendix E

Composition of Water + *n*-Butanol + P(VC_{12}ImBr) Systems

E.1 Composition of Water + *n*-Butanol + P(VC_{12}ImBr) Systems

Table E. 1: Equilibrium data for the water + *n*-butanol + P(VC_{12}ImBr) system at 30°C, each set of data resulting from samples with known total *n*-butanol content

	At equilibrium					
	Aqueous Phase (wt%)			Polymer Phase (wt%)		
Overall *n*BuOH content (wt%)	H_2O	*n*BuOH	P(VC_{12}ImBr)	H_2O	*n*BuOH	P(VC_{12}ImBr)
6.0	94.8	5.2	0	14.5	12.0	73.5
5.0	95.7	4.3	0	15.4	10.7	73.9
4.0	96.6	3.4	0	15.3	9.3	75.4
3.0	97.5	2.5	0	15.1	8.4	76.3
2.0	98.4	1.6	0	17.7	7.1	75.2
1.0	99.3	0.8	0	18.8	5.6	76.1

E.2 Recovery of *n*-Butanol in Organic Phase

The following is an example calculation for determining the organic phase mass fraction that was recovered, along with the amount of *n*-butanol in the organic phase, where the sample vial acts as the decanter as in the proposed set-up in Section 4.3. The known values and solubilities used for the calculations are from the sample recovered in Section 4.3.2 and are listed below.

Variable	Description	Value
$nBuOH_t$	Total *n*-butanol	1.22 g
H_2O_t	Total water	3.00 g
x_1	Aqueous phase mass	7.3 wt% *n*BuOH 92.7 wt% H_2O
x_2	Organic phase mass	79.7 wt% *n*BuOH 20.3 wt% H_2O
ρ_b	*n*-Butanol density	810 g/L
ρ_w	Water density	998 g/L

Using the total masses of *n*-butanol and water in the recovered sample, along with the solubility limit, the compositions of each phase were found with a set of equations.

Equation E.1:

$$(0.073)x_1 + (0.797)x_2 = 1.22\ g$$

Equation E.2:

$$(0.927)x_1 + (0.203)x_2 = 3.00\ g$$

Which is rearranged to be:

$$x_2 = \frac{3.00\ g - (0.927)x_1}{0.203}$$

Next, rearranged Equation E.2 is subbed into Equation E.1 to find the aqueous phase mass:

$$(0.073)x_1 + (0.797)\left(\frac{3.00\ g - 0.927x_1}{0.203}\right) = 1.22\ g$$

$$x_1 = 2.96\ g$$

Then, the organic phase mass was found by subbing the aqueous phase mass into Equation E.2:

$$x_2 = \frac{3.00\ g - (0.927)(2.96\ g)}{0.203} = 1.26\ g$$

Next, the mass fraction of the organic phase in the vial was found:

$$Organic\ phase\ in\ vial = \left(\frac{1.26\ g}{1.26\ g + 2.96\ g}\right)(100) = 29.9\ wt\%$$

Then, the mass and volume of *n*-butanol and water in each phase were found using the known solubility limits and densities:

$$Organic\ phase\ nBuOH = (1.26)(0.797) = 1.004\ g = 1.24\ mL$$

$$Organic\ phase\ water = (1.26)(0.203) = 0.256\ g = 0.257\ mL$$

$$Organic\ phase\ volume = 1.497\ mL$$

$$Aqueous\ phase\ nBuOH = (2.96)(0.073) = 0.216\ g = 0.267\ mL$$

$$Aqueous\ phase\ water = (2.96)(0.927) = 2.74\ g = 2.75\ mL$$

$$Aqueous\ phase\ volume = 3.017\ mL$$

Then, the organic phase volume fraction in the vial was found:

$$Organic\ phase\ volume = \left(\frac{1.467\ mL}{1.467\ mL + 3.017\ mL}\right) = 32.7\ vol\%$$

Finally, the amount of *n*-butanol in the organic phase in relation to the total amount of *n*-butanol recovered from P(VC_{12}ImBr) was found:

$$\%\ nBuOH\ in\ organic\ phase = \left(\frac{1.004\ g}{1.004\ g + 0.216\ g}\right)(100) = 82.3\%$$

Therefore, 82.3% of the *n*-butanol recovered from P(VC_{12}ImBr) would be separated in the decanter and sent to the distillation column for purification in the proposed setup.